mathematics

MDPI

Article

Mathematical Analysis of Multi-Route Tuberculosis Transmission with Airborne Environmental Reservoirs and Treatment Failure

Nada A. Almuallem

Department of Mathematics and Statistics, Faculty of Science, University of Jeddah, P.O. Box 80327, Jeddah 21589, Saudi Arabia; naalmouallim@uj.edu.sa

Abstract

Despite the availability of effective treatment, tuberculosis (TB) remains a major public health problem worldwide. Related factors that promote continued transmission include treatment failure, residual infectiousness during treatment, environmental contamination, and progression from latent to active TB in the absence of tuberculosis preventive treatment (TPT). This study aims to investigate the interplay of these factors with regard to TB transmission and identify intervention measures that can shift the disease from persistence to elimination. To achieve this objective, we formulate and analyze an SLIQTPR compartmental model that incorporates latent infection, preventive treatment of latently infected individuals, treatment of infectious individuals, treatment failure, residual infectiousness among treated individuals, and an environmental pathogen reservoir. The model accounts for both direct transmission from infectious and treated individuals and indirect transmission through environmental contamination. Positivity and boundedness of the model solutions are established, and the disease-free and endemic equilibria are characterized. The basic reproduction number, $\mathfrak{R}_0$, is derived using the next-generation matrix method and used to determine the threshold behavior of the model. Lyapunov function and LaSalle-invariance arguments are employed to establish the global asymptotic stability of the disease-free equilibrium when $\mathfrak{R}_0 \leq 1$ and of the endemic equilibrium when $\mathfrak{R}_0 > 1$. Normalized local and global sensitivity analyses are performed to identify the parameters exerting the greatest influence on TB transmission. In addition, an explicit threshold relationship between treatment failure and the residual infectiousness of treated individuals is derived to quantify their joint effect on the transition between disease elimination and persistence. Numerical simulations support the analytical findings and illustrate the effects of active treatment, TPT, and environmental pathogen clearance. The results indicate that TPT expansion, treatment efficacy improvement, treatment failure and residual infectiousness minimization, and speeding up environmental pathogen clearance may substantially decrease TB transmission. These results provide a quantitative basis for the development of integrated TB-control strategies that simultaneously target latent infection, treatment outcomes, and environmental transmission.

Keywords: tuberculosis; mathematical epidemiology; environmental transmission; treatment failure; preventive treatment; global asymptotic stability; sensitivity analysis; threshold analysis

MSC: 34D23; 37N25; 92D30; 34C60

Check for updates

Academic Editor: Till D. Frank

Received: 22 July 2026
Revised: 23 September 2026
Accepted: 1 October 2026
Published: 6 October 2026

Copyright: © 2026 by the author. Licensee MDPI, Basel, Switzerland. This article is an open access article distributed under the terms and conditions of the Creative Commons Attribution (CC BY) license.

1. Introduction

Mycobacterium tuberculosis is the cause behind tuberculosis (TB). When a person with pulmonary tuberculosis coughs, sneezes, speaks, or sings, they discharge infectious particles into the air. Extrapulmonary tuberculosis is a type of tuberculosis (TB), a disease that usually affects the lungs, but it can also affect other parts of the body. Once exposed, people usually become either latently infected with tuberculosis (LTBI) (asymptomatic and not transmissible) or develop active disease, which can continue to spread. The likelihood of development is highest in the first two years after infection and is much higher for HIV patients and for patients with compromised immune systems [1]. In spite of the availability of efficient diagnostic techniques and curative therapies, tuberculosis continues to be one of the major causes of mortality from a single infectious agent worldwide. The World Health Organization (WHO) projected that 10.7 million people—5.8 million men, 3.7 million women, and 1.2 million children—received a tuberculosis (TB) diagnosis in 2024. The disease is estimated to have killed 1.23 million people, of whom around 150,000 were HIV-positive [1].

Environmental factors such as humidity, poor ventilation, crowding, and poor indoor air quality can promote the persistence of infectious respiratory particulates and increase the risk of indirect TB transmission [2]. WHO recommends an integrated approach to infection prevention and control (IPC) that comprises standard administrative procedures, environmental control, and respiratory protection to reduce airborne transmission of M. tuberculosis. Environmental interventions that reduce the concentration of live airborne bacteria and hence the risk of illness include air filtration, upper-room ultraviolet germicidal irradiation (UVGI), and natural or mechanical ventilation [3]. Effective treatment of active TB is important in addition to these environmental measures to limit infectiousness. Patients may be infectious until therapy reduces the bacillary burden to a sufficiently low level. Delayed bacteriological conversion and inadequate or incomplete treatment may increase the duration of infectiousness and the risk of treatment failure, relapse, and drug resistance [1,4]. WHO also recommends TB preventive treatment (TPT) for people with latent TB infection, especially those at high risk of developing active TB disease, to reduce the risk of progression to active disease [1].

Mathematical models have been widely used for the understanding of TB transmission and the evaluation of different prevention and treatment strategies. Earlier work has considered important epidemiological processes such as latency, vaccination, treatment, relapse, reinfection, drug resistance, and optimal-control strategies. Liu and Zhang [5] developed an SVLIT model to investigate the effects of vaccination and treatment on TB transmission and analyzed its threshold dynamics. Yang et al. [6] studied two TB models with incomplete treatment in which treated individuals could return either to the latent compartment because of residual *Mycobacterium tuberculosis* or directly to the infectious compartment following treatment failure. Liu and Wang [7] considered treatment interruption and two latent stages, whereas Ullah et al. [8] examined efficient and incomplete treatment and the reduced infectiousness of treated individuals. Barrios et al. [9] formulated a synthesized TB model representing treatment abandonment. More recently, Onuorah et al. [10] generalized the model to include antibiotic resistance and explored how treatment failure promotes the persistence and transmission of resistant tuberculosis. Other mathematical work has considered relapse and reinfection [11], drug resistance [12,13], and optimal-control interventions [14]. Such studies have significantly improved the mathematical knowledge of TB transmission and control.

Preventive treatment for individuals with latent TB infection has also received increasing attention in mathematical modelling. Zhang et al. [15] formulated a model incorporating preventive treatment of latently infected individuals and reduced infectiousness among individuals receiving treatment for active TB. Their results demonstrated that increasing

preventive-treatment coverage could contribute to reducing TB transmission. Subsequently, Zhao et al. [16] developed a model of preventive treatment and vaccination strategies. The studies underscore the importance of reducing progression from latent infection to active disease. However, they did not simultaneously combine latent preventive treatment with an environmental pathogen reservoir and an explicit transition from the treated compartment back to the infectious compartment following treatment failure.

A separate group of mathematical models has investigated the contribution of environmental contamination to TB transmission. Li and Wang [17] developed an SVEIRB model incorporating environmental transmission, vaccination, and reinfection and showed that environmental control measures could contribute to TB elimination. Yulida et al. [18] identified mathematical models of TB that included environmental factors and emphasized the significance of environmental dynamics of pathogens. Recently, Ochieng et al. [19] studied a TB model incorporating environmental transmission and optimal-control interventions. Nevertheless, these environmental models do not simultaneously incorporate preventive treatment of latent infection, residual infectiousness during active treatment, and an explicit treatment-failure transition from the treated compartment to the infectious compartment.

The existing literature demonstrates that treatment failure, residual infectiousness, latent preventive treatment, and environmental transmission have previously been investigated either separately or in partial combinations. However, their joint influence on TB threshold dynamics remains insufficiently understood. Untreated infectious individuals may sustain environmental contamination through pathogen shedding, while individuals receiving active treatment may continue to transmit TB directly at a reduced rate before bacteriological conversion. Treatment failure may further sustain transmission by returning unsuccessfully treated individuals to the infectious compartment. Conversely, preventive treatment can reduce the progression of latently infected individuals to active disease. These interacting mechanisms provide a strong biological and epidemiological motivation for studying treatment outcomes, preventive treatment, and environmental transmission under the same mathematical framework. Motivated by this research gap, we formulate an SLIQTPR model that integrates three routes of TB transmission: direct transmission from untreated infectious individuals, reduced direct transmission from individuals receiving active treatment, and indirect transmission through an environmental pathogen reservoir. The model distinguishes preventive treatment of latent infection from active TB treatment and incorporates both successful treatment and treatment failure, through which unsuccessfully treated individuals return to the infectious compartment. The environmental compartment accounts for pathogen shedding by untreated infectious individuals and pathogen clearance from the environment. The novelty of the proposed model lies not in these mechanisms individually, but in integrating latent TB preventive treatment, residual infectiousness during active treatment, an explicit treatment-failure pathway, and environmental transmission within a single analytically tractable framework. This structure enables us to investigate their combined effects on TB elimination and persistence. Furthermore, an explicit critical-threshold relationship between the treatment-failure rate and the relative infectiousness of treated individuals is derived to identify the combinations of these factors that lead either to disease elimination or continued disease persistence.

The remainder of the paper is organized in this manner. Section 2 presents the formulation of the proposed SLIQTPR tuberculosis model. Section 3 is devoted to the mathematical analysis of the model, where the positivity and boundedness of solutions are established, the disease-free and endemic equilibria are derived, the basic reproduction number, $\mathfrak{R}_0$, is obtained using the next-generation matrix approach, and the global asymptotic stability of both equilibria is established. Section 4 presents the sensitivity analysis of $\mathfrak{R}_0$ to identify the most influential epidemiological parameters. It also provides an analytical investigation

of the critical threshold relationship between the treatment-failure rate and the residual infectiousness parameter. Numerical simulations are provided in Section 5 to verify the theoretical results and to study the effect of TB preventative treatment, active TB treatment, and environmental pathogen clearance on the infectious population and environmental pathogen concentration. Section 6 summarizes the main findings, gives recommendations for future research, and concludes this work.

2. TB Model Formulation

To explain the mechanics of TB transmission, we propose seven epidemiological compartments, namely susceptible (X_S), latent (X_L), infectious (X_I), individuals receiving preventive treatment for latent tuberculosis infection (LTBI) (X_Q), individuals receiving active TB treatment (X_T), recovered (X_R), and the airborne environmental pathogen load (X_P). The model is formulated based on the following biological assumptions:

- The susceptible population (X_S), described by Equation (1a), is recruited into the population at rate Π and experiences natural mortality at rate μ_S. Susceptible individuals acquire tuberculosis through three transmission routes: direct contact with infectious individuals at rate λ_I, direct contact with actively infectious individuals receiving treatment at the reduced rate $\lambda_T = \eta\lambda_I$, where $0 < \eta < 1$, and indirect exposure to viable airborne *M. tuberculosis* at rate λ_P. Actively infectious individuals receiving treatment (X_T) are assumed to be less infectious than untreated infectious individuals (X_I) because treatment reduces bacterial shedding and infectivity. Consequently, transmission from treated individuals is modeled by the reduced transmission rate $\lambda_T = \eta\lambda_I$, following the modeling approaches of Li et al. [8]. Accordingly, the force of infection incorporates both direct and environmental transmission.
- Newly infected individuals with *M. tuberculosis* enter the latent compartment (X_L) described by Equation (1b) in which they are infected but not infectious. They may progress to active tuberculosis at rate κ_L, initiate tuberculosis preventive treatment at rate q_L [15], or experience natural mortality at rate μ_L.
- The infectious compartment (X_I), governed by Equation (1c), consists of individuals with active pulmonary tuberculosis who are capable of transmitting infection. Individuals in this compartment receive treatment for active tuberculosis at a rate of κ_I and are removed through the combined natural and disease-induced mortality rate μ_I.
- Some individuals with latent tuberculosis infection (LTBI) initiate tuberculosis preventive treatment and enter the preventive-treatment compartment (X_Q), represented by Equation (1d). Since individuals with LTBI do not have active tuberculosis, they are assumed not to contribute to disease transmission. Individuals in this compartment either successfully complete preventive treatment at rate γ_Q, thereby moving to the recovered compartment, or experience natural mortality at rate μ_Q [15].
- The treated compartment (X_T), represented by Equation (1e), consists of individuals receiving treatment for active tuberculosis. As previously assumed, treated individuals retain residual infectiousness and therefore contribute to disease transmission at a reduced rate [8]. They either successfully complete treatment at rate γ_T, experience the combined natural and disease-induced mortality rate μ_T, or undergo treatment failure at rate ϕ, returning directly to the infectious compartment. Consistent with the updated WHO treatment-outcome definitions, this transition represents treatment failure rather than relapse following successful treatment [1,4].
- The environmental compartment (X_P), represented by Equation (1f), describes the environmental TB pathogen load at time t. The environmental bacterial load increases through continuous pathogen shedding by infectious individuals at rate α and de-

creases through environmental clearance at rate ω, including ventilation, air exchange, and natural bacterial decay [17].

- Finally, the recovered compartment (X_R) represented by Equation (1g) consists of individuals who have successfully completed either preventive treatment or treatment for active tuberculosis. The recovery parameters are estimated from the average duration of treatment according to current WHO recommendations. The duration of tuberculosis preventive treatment (TPT) for latent tuberculosis infection (LTBI) is assumed to range from 3 to 6 months. Accordingly, the corresponding per capita treatment-completion rate is $\gamma_Q \in [1/0.5, 1/0.25] = [2, 4]$ year^{-1} [20]. A representative baseline value within this range is selected as $\gamma_Q = 3$ year^{-1}, corresponding to an average treatment duration of four months. For active tuberculosis, a conventional six-month treatment duration is assumed, giving the recovery rate $\gamma_T = 1/0.5 = 2$ year^{-1} [21]. The biological interpretation of the model parameters together with their baseline values is summarized in Tables 1 and 2.

Under these assumptions, the transmission dynamics of tuberculosis are governed by the following system of ordinary differential equations:

$$\frac{dX_S(t)}{dt} = \Pi - (\lambda_I X_I + \lambda_T X_T + \lambda_P X_P)X_S - \mu_S X_S, \tag{1a}$$

$$\frac{dX_L(t)}{dt} = (\lambda_I X_I + \lambda_T X_T + \lambda_P X_P)X_S - (\kappa_L + q_L + \mu_L)X_L, \tag{1b}$$

$$\frac{dX_I(t)}{dt} = \kappa_L X_L + \phi X_T - (\kappa_I + \mu_I)X_I, \tag{1c}$$

$$\frac{dX_Q(t)}{dt} = q_L X_L - (\gamma_Q + \mu_Q)X_Q, \tag{1d}$$

$$\frac{dX_T(t)}{dt} = \kappa_I X_I - (\phi + \gamma_T + \mu_T)X_T, \tag{1e}$$

$$\frac{dX_P(t)}{dt} = \alpha X_I - \omega X_P, \tag{1f}$$

$$\frac{dX_R(t)}{dt} = \gamma_Q X_Q + \gamma_T X_T - \mu_R X_R, \tag{1g}$$

where $\lambda_T = \eta\lambda_I,\ 0 < \eta < 1$ and the starting conditions are

$$\begin{aligned} &X_S(0) \geq 0,\ X_L(0) \geq 0,\ X_I(0) \geq 0,\ X_Q(0) \geq 0, \\ &X_T(0) \geq 0,\ \ X_P(0) \geq 0 \ \text{ and } \ X_R(0) \geq 0. \end{aligned} \tag{2}$$

The model's parameters are positive and constant. The corresponding flow diagram is shown in Figure 1, and the biological meanings of the model variables and parameters are summarized in Tables 1 and 2.

Table 1. Explanation of the model's variables.

Variable	Description
X_S	Susceptible class
X_L	Latent class
X_I	Infectious class
X_Q	Preventive treatment for latent TB infection class
X_T	Treatment for active infectious TB class
X_P	Airborne TB pathogen class
X_R	Recovered class

Table 2. Parameter descriptions, baseline values, units, and references used in the proposed model (1). References marked by "*" and "**" correspond to parameter values calculated from the recommended treatment durations.

Param.	Description	Value	Unit	Ref.
Π	Recruitment rate	$10,000/70$	Individuals year^{-1}	[6,19]
λ_I	Transmission rate due to infectious individuals, X_I	5×10^{-5}	(Individuals year)$^{-1}$	[6]
λ_P	Airborne transmission coefficient, X_P	1×10^{-5}	(Pathogen year)$^{-1}$	[17]
η	Relative infectiousness of treated individuals	0.1	–	[8]
κ_L	Translation rate from X_L to X_I	0.129	year^{-1}	[22]
q_L	Preventive treatment initiation rate	0.3	year^{-1}	[15]
κ_I	Treatment rate of infectious individuals	0.5	year^{-1}	[15]
ϕ	Treatment failure leading to active TB	0.225	year^{-1}	[6]
α	MTB shedding rate by infectious individuals	142.0803	$\frac{\text{Pathogen}}{\text{individual} \cdot \text{year}}$	[19]
ω	Clearance rate of environmental pathogens	8.073	year^{-1}	[19]
μ_S	Natural mortality rate of susceptible individuals	$1/70$	year^{-1}	[6]
μ_L	Natural mortality rate of latent individuals	$1/70$	year^{-1}	[6]
μ_I	Combined natural and disease-induced mortality rate of X_I	$1/70 + 0.3$	year^{-1}	[6]
μ_Q	Natural mortality rate of X_Q	$1/70$	year^{-1}	[6]
μ_T	Combined natural and disease-induced mortality rate of X_T	$1/70 + 0.05$	year^{-1}	[6]
μ_R	Natural mortality rate of recovered individuals	$1/70$	year^{-1}	[6]
γ_Q	Completion rate of preventive treatment	3	year^{-1}	* [20]
γ_T	Treatment success rate	2	year^{-1}	** [21]

References marked by * and ** were calculated from the corresponding treatment durations as $\gamma_Q = 1/(4/12) = 3$ year^{-1} [20] and $\gamma_T = 1/(6/12) = 2$ year^{-1} [21], respectively.

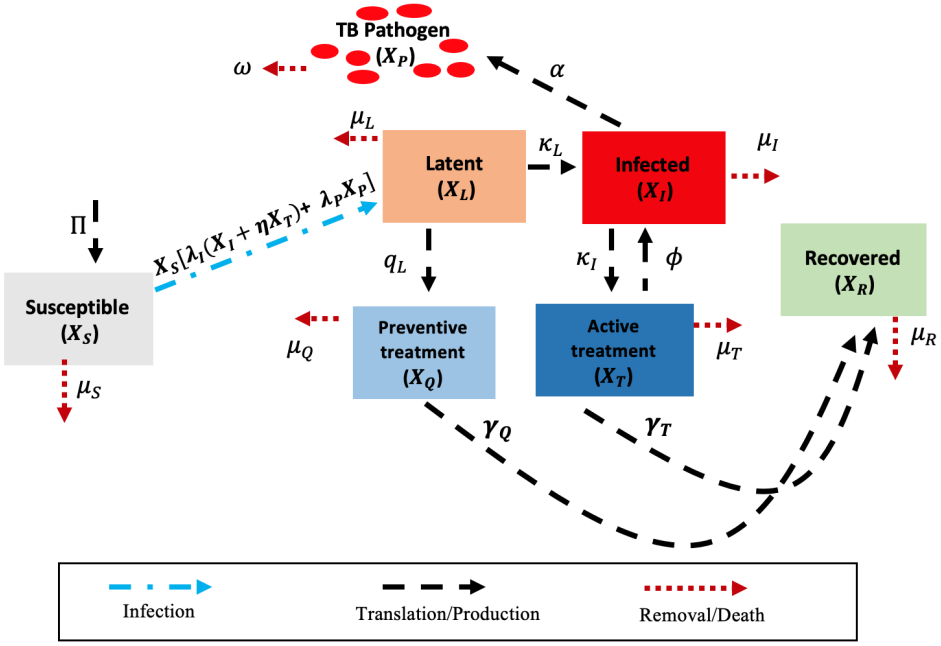


Figure 1. Flow diagram of the proposed tuberculosis transmission model (1). Susceptible individuals (X_S) become latently infected (X_L) through direct contact with infectious (X_I) or treated individuals with residual infectiousness (X_T), as well as through exposure to environmental pathogens (X_P). Latent individuals either progress to active tuberculosis at rate (κ_L) or initiate preventive treatment at rate (q_L). Individuals in the preventive treatment class (X_Q) recover at a rate (γ_Q). Infectious individuals receive treatment at rate (κ_I), while treated individuals may experience treatment failure and return to the infectious class at rate (ϕ) or recover at rate (γ_T). Infectious individuals shed *Mycobacterium tuberculosis* into the environment at rate (α), and environmental pathogens are removed at rate (ω). All compartments are subject to their corresponding mortality rates.

3. The TB Model's Mathematical Analysis

3.1. Boundedness and Non-Negativity

In this part, we demonstrate the boundedness and positivity for the solutions to model (1) given initial conditions (2).

Proposition 1. *Let* $(X_S(t), X_L(t), X_I(t), X_Q(t), X_T(t), X_P(t), X_R(t))$ *be a solution of the model (1) satisfying the initial conditions (2), then the compact set*

$$\Omega_T = \left\{ (X_S, X_L, X_I, X_Q, X_T, X_P, X_R) \in \mathbb{R}^7_+ : 0 \leq X_N \leq \frac{\Pi}{\mu}; 0 \leq X_P \leq \frac{\Pi\alpha}{\mu\omega} \right\}$$

is positively invariant for the model (1). In particular, every solution with initial state in Ω_T *remains in* Ω_T *for all* $t \geq 0$.

Proof. We obtain from model (1)

$$\begin{aligned}
\left.\frac{dX_S(t)}{dt}\right|_{X_S \to 0} &= \Pi > 0, \\
\left.\frac{dX_L(t)}{dt}\right|_{X_L \to 0} &= [\lambda_I X_I + \lambda_T X_T + \lambda_P X_P] X_S \geq 0, \\
\left.\frac{dX_I(t)}{dt}\right|_{X_I \to 0} &= \kappa_L X_L + \phi X_T \geq 0, \\
\left.\frac{dX_Q(t)}{dt}\right|_{X_Q \to 0} &= q_L X_L \geq 0, \\
\left.\frac{dX_T(t)}{dt}\right|_{X_T \to 0} &= \kappa_I X_I \geq 0, \\
\left.\frac{dX_P(t)}{dt}\right|_{X_P \to 0} &= \alpha X_I \geq 0, \\
\left.\frac{dX_R(t)}{dt}\right|_{X_R \to 0} &= \gamma_Q X_Q + \gamma_T X_T \geq 0.
\end{aligned} \tag{3}$$

Hence, we can see that $X_S, X_L, X_I, X_Q, X_T, X_P \geq 0$ for all $t \geq 0$. Furthermore, X_R is non-negative, since

$$X_R(t) = e^{-\mu_R t} X_R(0) + \int_0^t e^{-\mu_R (t-\eta)} (\gamma_Q X_Q(\eta) + \gamma_T X_T(\eta)) d\eta.$$

Next, we define a function X_N is the total number of people, then

$$X_N(t) = X_S(t) + X_L(t) + X_I(t) + X_Q(t) + X_T(t) + X_R(t).$$

Then, we have the following after differentiation:

$$\begin{aligned}
\frac{dX_N(t)}{dt} =& \Pi - \mu_S X_S - \mu_L X_L - \mu_I X_I - \mu_Q X_Q - \mu_T X_T - \mu_R X_R \\
\leq& \Pi - \mu X_N,
\end{aligned}$$

where $\mu = min(\mu_S, \mu_L, \mu_I, \mu_Q, \mu_T, \mu_R)$. Hence,

$$X_N(t) \leq e^{-\mu t} \left(X_N(0) - \frac{\Pi}{\mu} \right) + \frac{\Pi}{\mu}.$$

This results in $0 \leq X_N(t) \leq \frac{\Pi}{\mu}$ if $X_N(0) \leq \frac{\Pi}{\mu}$. Given that every variable is non-negative, then $0 \leq X_S, X_L, X_I, X_Q, X_T, X_R \leq \frac{\Pi}{\mu}$, for all $t \geq 0$, if $X_S(0) + X_L(0) + X_I(0) + X_Q(0) + X_T(0) + X_R(0) \leq \frac{\Pi}{\mu}$. Moreover,

$$\frac{dX_P(t)}{dt} = \alpha X_I - \omega X_P \leq \frac{\Pi\alpha}{\mu} - \omega X_P.$$

Then $0 \leq X_P(t) \leq \frac{\Pi\alpha}{\mu\omega}$, if $X_P(0) \leq \frac{\Pi\alpha}{\mu\omega}$, for all $t \geq 0$. □

3.2. Basic Reproduction Number and the Equilibria

The basic reproduction number and the model's equilibria (1) are found in this section.

Proposition 2. *There is a basic reproduction number $\mathfrak{R}_0 > 0$ for model (1) such that*

(i) if $\mathfrak{R}_0 \leq 1$, then there exists a unique non-negative TB-free equilibrium $\mathcal{T}_0 \in \Omega_T$;

(ii) if $\mathfrak{R}_0 > 1$, then there exist two non-negative equilibria: the TB-free equilibrium $\mathcal{T}_0 \in \Omega_T$ and the endemic equilibrium $\mathcal{T}^* \in \Omega_T^\circ$, where Ω_T° is the interior of Ω_T.

Proof. (i) Model (1) equilibrium points satisfy the following requirements:

$$0 = \Pi - [\lambda_I X_I + \lambda_T X_T + \lambda_P X_P] X_S - \mu_S X_S, \tag{4a}$$
$$0 = (\lambda_I X_I + \lambda_T X_T + \lambda_P X_P) X_S - e_1 X_L, \tag{4b}$$
$$0 = \kappa_L X_L + \phi X_T - e_2 X_I, \tag{4c}$$
$$0 = q_L X_L - e_3 X_Q, \tag{4d}$$
$$0 = \kappa_I X_I - e_4 X_T, \tag{4e}$$
$$0 = \alpha X_I - \omega X_P, \tag{4f}$$
$$0 = \gamma_Q X_Q + \gamma_T X_T - \mu_R X_R, \tag{4g}$$

where

$$e_1 = \kappa_L + q_L + \mu_L, \;\; e_2 = \kappa_I + \mu_I, \;\; e_3 = \gamma_Q + \mu_Q \;\text{ and }\; e_4 = \phi + \gamma_T + \mu_T. \tag{5}$$

It is easy to show from Equation (4a–g) that a TB-free equilibrium $\mathcal{T}_0$ occurs when the disease is not present in the population. The point $\mathcal{T}_0 = (X_S^0, 0, 0, 0, 0, 0, 0) = \left(\frac{\Pi}{\mu_S}, 0, 0, 0, 0, 0, 0\right)$ is obtained by substituting X_L or $X_I = 0$ into Equation (4a–g). The basic reproduction number, $\mathfrak{R}_0$, of the TB model (1) is determined at the TB-free equilibrium point $\mathcal{T}_0$ as follows:

Basic reproduction number ($\mathfrak{R}_0$):

A key parameter for evaluating the transmission of illness within a population is the basic reproduction number, denoted as $\mathfrak{R}_0$. This measure shows the likelihood that tuberculosis will either go extinct or persist in the population. Here, we use the procedure described in [23] to determine the formulation of the basic reproduction number. The two matrices that follow show the non-linear terms that correspond to the new disease $\mathcal{D}$ and the outflow $\mathcal{V}$ based on the infected classes in model (1), arranged by X_L, X_I, X_Q, X_T, and X_P:

$$\mathcal{D} = \begin{pmatrix} [\lambda_I \mathrm{X_I} + \lambda_T \mathrm{X_T} + \lambda_P \mathrm{X_P}]\mathrm{X_S} \\ 0 \\ 0 \\ 0 \\ 0 \end{pmatrix},$$

$$\mathcal{V} = \begin{pmatrix} e_1 \mathrm{X_L} \\ -\kappa_L \mathrm{X_L} - \phi \mathrm{X_T} + e_2 \mathrm{X_I} \\ -q_L \mathrm{X_L} + e_3 \mathrm{X_Q} \\ -\kappa_I \mathrm{X_I} + e_4 \mathrm{X_T} \\ -\alpha \mathrm{X_I} + \omega \mathrm{X_P} \end{pmatrix}.$$

At the TB-free equilibrium point $\mathcal{T}_0$, the derivatives of $\mathcal{D}$ and $\mathcal{V}$ are given by

$$\bar{\mathcal{D}} = \begin{pmatrix} 0 & \lambda_I \mathrm{X_S^0} & 0 & \lambda_T \mathrm{X_S^0} & \lambda_P \mathrm{X_S^0} \\ 0 & 0 & 0 & 0 & 0 \\ 0 & 0 & 0 & 0 & 0 \\ 0 & 0 & 0 & 0 & 0 \\ 0 & 0 & 0 & 0 & 0 \end{pmatrix},$$

$$\bar{\mathcal{V}} = \begin{pmatrix} e_1 & 0 & 0 & 0 & 0 \\ -\kappa_L & e_2 & 0 & -\phi & 0 \\ -q_L & 0 & e_3 & 0 & 0 \\ 0 & -\kappa_I & 0 & e_4 & 0 \\ 0 & -\alpha & 0 & 0 & \omega \end{pmatrix}.$$

Therefore, $\mathfrak{R}_0$ may be found using $\rho(\bar{\mathcal{D}}\bar{\mathcal{V}}^{-1})$, where $\rho(F)$ is the spectral radius of matrix F. Following that, we obtain

$$\mathfrak{R}_0 = \frac{\kappa_L \mathrm{X_S^0}(\lambda_I \omega e_4 + \lambda_T \omega \kappa_I + \alpha \lambda_P e_4)}{\omega e_1 (e_2 e_4 - \kappa_I \phi)}. \tag{6}$$

Consequently, it is possible to rewrite the basic reproduction number, $\mathfrak{R}_0$, in terms of λ_I, using the relation $\lambda_T = \eta \lambda_I$, as follows:

$$\mathfrak{R}_0 = \underbrace{\frac{\mathrm{X_S^0} \kappa_L \lambda_I e_4}{e_1(e_4 e_2 - \kappa_I \phi)}}_{\mathfrak{R}_I} + \underbrace{\frac{\mathrm{X_S^0} \kappa_L \eta \kappa_I \lambda_I}{e_1(e_4 e_2 - \kappa_I \phi)}}_{\mathfrak{R}_T} + \underbrace{\frac{\mathrm{X_S^0} \kappa_L \alpha \lambda_P e_4}{e_1(e_4 e_2 - \kappa_I \phi)\omega}}_{\mathfrak{R}_P}. \tag{7}$$

The first term, $\mathfrak{R}_I$, represents the expected number of secondary tuberculosis infections generated through direct transmission from infectious individuals during their average infectious period. In addition, the second term, $\mathfrak{R}_T$, represents the contribution of treated individuals who continue to transmit the disease. Finally, $\mathfrak{R}_P$ represents the contribution of environmental transmission through viable *Mycobacterium tuberculosis* that is present in the environment. This term accounts for infections acquired from exposure to contaminated air containing infectious bacteria. Thus the basic reproduction number is a sum of the contributions of infectious individuals, treated individuals, and environmental transmission through pathogen reservoirs. When $\mathfrak{R}_0 \leq 1$, disease elimination is achieved, whereas when $\mathfrak{R}_0 > 1$, transmission is sustained.

(ii) To get the TB model's endemic equilibrium point (TB-endemic), $\mathcal{T}^*$ with $\mathcal{T}_0$, let $\mathcal{T}^* = (\tilde{X}_S, \tilde{X}_L, \tilde{X}_I, \tilde{X}_Q, \tilde{X}_T, \tilde{X}_P, \tilde{X}_R)$ be the endemic equilibrium point of model (1). By solving Equations (4a–g), we derive the following formulas for the $\mathcal{T}^*$:

$$\tilde{X}_S = \frac{\Pi}{A_1 + \mu_S}, \quad \tilde{X}_L = \frac{A_1 \Pi}{e_1(A_1 + \mu_S)}, \tag{8}$$

$$\tilde{X}_I = \frac{e_4 \kappa_L \tilde{X}_L}{e_2 e_4 - \phi \kappa_I}, \quad \tilde{X}_Q = \frac{q_L \tilde{X}_L}{e_3}, \tag{9}$$

$$\tilde{X}_T = \frac{\kappa_I \kappa_L \tilde{X}_L}{e_2 e_4 - \phi \kappa_I}, \quad \tilde{X}_P = \frac{\alpha e_4 \kappa_L \tilde{X}_L}{\omega(e_2 e_4 - \phi \kappa_I)}, \tag{10}$$

$$\tilde{X}_R = \frac{(e_2 e_4 \gamma_Q q_L + e_3 \gamma_T \kappa_L \kappa_I - \phi \gamma_Q \kappa_I q_L)\tilde{X}_L}{\mu_R e_3 (e_2 e_4 - \phi \kappa_I)}, \tag{11}$$

where,

$$A_1 = \lambda_I \tilde{X}_I + \lambda_T \tilde{X}_T + \lambda_P \tilde{X}_P, \tag{12}$$

denotes the infectious force assessed at the endemic equilibrium (i.e., $A_1 > 0$), while the quantities e_1, e_2, e_3, and e_4 are defined in (5). To express the endemic equilibrium in terms of the basic reproduction number, we first substitute the expressions for $\tilde{X}_I$, $\tilde{X}_T$, and $\tilde{X}_P$ from Equations (9) and (10) into Equation (12). Thus,

$$A_1 = \frac{\kappa_L \tilde{X}_L}{e_2 e_4 - \phi \kappa_I} \left(e_4 \lambda_I + \kappa_I \lambda_T + \frac{\alpha e_4 \lambda_P}{\omega} \right).$$

For simplicity, define

$$K = \frac{\kappa_L}{e_2 e_4 - \phi \kappa_I} \left(e_4 \lambda_I + \kappa_I \lambda_T + \frac{\alpha e_4 \lambda_P}{\omega} \right).$$

Then,

$$A_1 = K \tilde{X}_L. \tag{13}$$

The first equilibrium equation gives

$$\tilde{X}_S = \frac{\Pi}{\mu_S + K \tilde{X}_L}. \tag{14}$$

Moreover, the second equilibrium equation satisfies

$$A_1 \tilde{X}_S = e_1 \tilde{X}_L.$$

Using Equation (13), we obtain

$$K \tilde{X}_L \tilde{X}_S = e_1 \tilde{X}_L.$$

Since $\tilde{X}_L > 0$ at the endemic equilibrium, it follows that

$$K \tilde{X}_S = e_1, \qquad \text{and hence} \qquad \tilde{X}_S = \frac{e_1}{K}.$$

From the definition of the basic reproduction number,

$$\mathfrak{R}_0 = \frac{X_S^0 K}{e_1},$$

and therefore,

$$K = \frac{e_1 \mathfrak{R}_0}{X_S^0}.$$

Consequently,

$$\tilde{X}_S = \frac{e_1}{K} = \frac{X_S^0}{\mathfrak{R}_0}.$$

Next, substituting

$$\tilde{X}_S = \frac{X_S^0}{\mathfrak{R}_0} \quad \text{and} \quad K = \frac{e_1 \mathfrak{R}_0}{X_S^0},$$

into Equation (14) gives

$$\frac{X_S^0}{\mathfrak{R}_0} = \frac{\Pi}{\mu_S + \frac{e_1 \mathfrak{R}_0}{X_S^0} \tilde{X}_L}.$$

Using $X_S^0 = \Pi/\mu_S$ and solving for $\tilde{X}_L$, we obtain

$$\tilde{X}_L = \frac{\mu_S X_S^0 (\mathfrak{R}_0 - 1)}{e_1 \mathfrak{R}_0}.$$

Thus, Equation (15) follows. Finally, substituting this expression for $\tilde{X}_L$ into Equations (9)–(11) yields the remaining endemic-equilibrium components given in Equations (16)–(18).

$$\tilde{X}_S = \frac{X_S^0}{\mathfrak{R}_0}, \quad \tilde{X}_L = \frac{\mu_S X_S^0 (\mathfrak{R}_0 - 1)}{e_1 \mathfrak{R}_0}, \tag{15}$$

$$\tilde{X}_I = \frac{e_4 \mu_S \omega (\mathfrak{R}_0 - 1)}{\omega e_4 \lambda_I + \kappa_I \omega \lambda_T + \alpha e_4 \lambda_P}, \quad \tilde{X}_Q = \frac{q_L \mu_S X_S^0 (\mathfrak{R}_0 - 1)}{e_1 e_3 \mathfrak{R}_0}, \tag{16}$$

$$\tilde{X}_T = \frac{\kappa_I \mu_S \omega (\mathfrak{R}_0 - 1)}{\omega e_4 \lambda_I + \kappa_I \omega \lambda_T + \alpha e_4 \lambda_P}, \quad \tilde{X}_P = \frac{\mu_S \alpha e_4 (\mathfrak{R}_0 - 1)}{\omega e_4 \lambda_I + \kappa_I \omega \lambda_T + \alpha e_4 \lambda_P}, \tag{17}$$

$$\tilde{X}_R = \frac{\mu_S \omega (\mathfrak{R}_0 - 1)(e_2 e_4 q_L \gamma_Q + e_3 \kappa_L \kappa_I \gamma_T - \phi \kappa_I q_L \gamma_Q)}{\mu_R e_3 \kappa_L (\omega e_4 \lambda_I + \kappa_I \omega \lambda_T + \alpha e_4 \lambda_P)}. \tag{18}$$

The TB-endemic equilibrium $\mathcal{T}^*$ will dominate the system if $\mathfrak{R}_0 > 1$, meaning that the infection will persist in the population for a considerable amount of time (becoming endemic).

We now prove that $\mathcal{T}_0 \in \Omega_T$ and $\mathcal{T}^* \in \Omega_T^\circ$. Clearly $\mathcal{T}_0 \in \Omega_T$. According to Equations (1a–g) at equilibrium state, we have

$$\mu_S \tilde{X}_S + \mu_L \tilde{X}_L + \mu_I \tilde{X}_I + \mu_Q \tilde{X}_Q + \mu_T \tilde{X}_T + \mu_R \tilde{X}_R = \Pi. \tag{19}$$

Since $\mathfrak{R}_0 > 1$, then $\tilde{X}_S$, $\tilde{X}_L$, $\tilde{X}_I$, $\tilde{X}_Q$, $\tilde{X}_T$ and $\tilde{X}_R$ are all positive and

$$\begin{aligned}
\mu_S \tilde{X}_S < \Pi &\Longrightarrow \tilde{X}_S < \frac{\Pi}{\mu_S} \leq \frac{\Pi}{\mu}, \\
\mu_L \tilde{X}_L < \Pi &\Longrightarrow \tilde{X}_L < \frac{\Pi}{\mu_L} \leq \frac{\Pi}{\mu}, \\
\mu_I \tilde{X}_I < \Pi &\Longrightarrow \tilde{X}_I < \frac{\Pi}{\mu_I} \leq \frac{\Pi}{\mu}, \\
\mu_Q \tilde{X}_Q < \Pi &\Longrightarrow \tilde{X}_Q < \frac{\Pi}{\mu_Q} \leq \frac{\Pi}{\mu}, \\
\mu_T \tilde{X}_T < \Pi &\Longrightarrow \tilde{X}_T < \frac{\Pi}{\mu_T} \leq \frac{\Pi}{\mu}, \\
\mu_R \tilde{X}_R < \Pi &\Longrightarrow \tilde{X}_R < \frac{\Pi}{\mu_R} \leq \frac{\Pi}{\mu}.
\end{aligned}$$

From Equation (1f), we have

$$\omega\tilde{X}_P = \alpha\tilde{X}_I < \frac{\alpha\Pi}{\mu_I} \Longrightarrow \tilde{X}_P < \frac{\alpha\Pi}{\omega\mu_I} \leq \frac{\alpha\Pi}{\omega\mu}$$

It follows that $\mathcal{T}^* \in \Omega_T^\circ$. □

3.3. Global Stability Analysis

In this part, we use LaSalle's invariance principle and the direct Lyapunov technique to investigate the global stability of the two equilibria of model (1). Throughout the article, the following function will be used. $H : (0,\infty) \to [0,\infty)$ as:

$$H(g) = g - 1 - \ln g. \tag{20}$$

It is clear that $H(g) \geq 0$ for any $g > 0$ and $H(g) = 0$ if and only if $g = 1$, where $g = g(t)$ for any $g \in (X_S, X_L, X_I, X_Q, X_T, X_P, X_R)$.

3.3.1. Global Stability for the TB-Free Equilibrium Point $\mathcal{T}_0$

Theorem 1. *The TB-free equilibrium point $\mathcal{T}_0$ is globally asymptotically stable (GAS) in Ω_T if $\mathfrak{R}_0 \leq 1$, and otherwise unstable.*

Proof. Suppose the function of Lyapunov is

$$U_0 = X_S^0 H\left(\frac{X_S}{X_S^0}\right) + X_L + \frac{e_1\mathfrak{R}_0}{\kappa_L}X_I + \left(\frac{\kappa_L X_S^0\lambda_T + \phi e_1\mathfrak{R}_0}{e_4\kappa_L}\right)X_T + \frac{\lambda_P X_S^0}{\omega}X_P, \tag{21}$$

where e_1, e_2, e_3, and e_4 are defined in (5). Differentiating U_0 with respect to time gives

$$\frac{dU_0}{dt} = \left(1 - \frac{X_S^0}{X_S}\right)\dot{X}_S + \dot{X}_L + \frac{e_1\mathfrak{R}_0}{\kappa_L}\dot{X}_I + \left(\frac{\kappa_L X_S^0\lambda_T + \phi e_1\mathfrak{R}_0}{e_4\kappa_L}\right)\dot{X}_T + \frac{\lambda_P X_S^0}{\omega}\dot{X}_P. \tag{22}$$

Substituting the governing equations for $\dot{X}_S$, $\dot{X}_L$, $\dot{X}_I$, $\dot{X}_T$ and $\dot{X}_P$ yields

$$\begin{aligned}\frac{dU_0}{dt} = {} & \left(1 - \frac{X_S^0}{X_S}\right)(\Pi - (\lambda_I X_I + \lambda_T X_T + \lambda_P X_P)X_S - \mu_S X_S) \\ & + (\lambda_I X_I + \lambda_T X_T + \lambda_P X_P)X_S - e_1 X_L + \frac{e_1\mathfrak{R}_0}{\kappa_L}(\kappa_L X_L + \phi X_T - e_2 X_I) \\ & + \left(\frac{\kappa_L X_S^0\lambda_T + \phi e_1\mathfrak{R}_0}{e_4\kappa_L}\right)(\kappa_I X_I - e_4 X_T) + \frac{\lambda_P X_S^0}{\omega}(\alpha X_I - \omega X_P).\end{aligned} \tag{23}$$

By substituting $\Pi = \mu_S X_S^0$ and simplifying the resulting expression, we obtain

$$\frac{dU_0}{dt} = \frac{-\mu_S(X_S - X_S^0)^2}{X_S} + e_1(\mathfrak{R}_0 - 1)X_L. \tag{24}$$

Since $\frac{dU_0}{dt} \leq 0$ whenever $\mathfrak{R}_0 \leq 1$ for all $X_S, X_L > 0$, it follows that $\frac{dU_0}{dt} = 0$ if and only if $X_S = X_S^0$ and $X_L = 0$. Define the set $\Gamma = \{(X_S, X_L, X_I, X_Q, X_T, X_P, X_R) \in \Omega_T : X_S = X_S^0, X_L = 0\}$. From the model equations, if $X_L = 0$, then $\dot{X}_L = 0$, and from Equation (1b) we have $0 = \lambda_I X_I + \lambda_T X_T + \lambda_P X_P$. Since $X_I \geq 0$, $X_T \geq 0$ and $X_P \geq 0$, it follows that $X_I = X_T = X_P = 0$. Finally, $\dot{X}_Q = -e_3 X_Q$ and $\dot{X}_R = -\mu_r X_R$ it follows that $X_Q \to 0$ and $X_R \to 0$ as $t \to \infty$. Hence, the largest compact invariant set of Γ is the singleton set $\{\mathcal{T}_0\}$, by LaSalle's Invariance Principle [24], the TB-free equilibrium point $\mathcal{T}_0$ is globally asymptotically stable whenever $\mathfrak{R}_0 \leq 1$. □

The above result indicates that the disease can be eliminated from the population if and only if $\mathfrak{R}_0 \leq 1$.

3.3.2. Global Stability for TB-Endemic Equilibrium Point $\mathcal{T}^*$

Theorem 2. *The TB-endemic equilibrium point $\mathcal{T}^*$ is globally asymptotically stable (GAS) in Ω_T° if $\mathfrak{R}_0 > 1$, and otherwise unstable.*

Proof. To show that the endemic equilibrium is GAS, we consider the following Lyapunov function:

$$U_1 = \tilde{X}_S H\left(\frac{X_S}{\tilde{X}_S}\right) + \tilde{X}_L H\left(\frac{X_L}{\tilde{X}_L}\right) + A\tilde{X}_I H\left(\frac{X_I}{\tilde{X}_I}\right) + B\tilde{X}_T H\left(\frac{X_T}{\tilde{X}_T}\right) + C\tilde{X}_P H\left(\frac{X_P}{\tilde{X}_P}\right),$$

where A, B and C are positive constants to be determined later, and e_1, e_2, e_3, and e_4 are defined in (5). We compute $\frac{dU_1}{dt}$ along the model's trajectories as

$$\begin{aligned}\frac{dU_1}{dt} &= \left(1 - \frac{\tilde{X}_S}{X_S}\right)(\Pi - (\lambda_I X_I + \lambda_T X_T + \lambda_P X_P)X_S - \mu_S X_S) \\ &+ \left(1 - \frac{\tilde{X}_L}{X_L}\right)((\lambda_I X_I + \lambda_T X_T + \lambda_P X_P)X_S - e_1 X_L) \\ &+ A\left(1 - \frac{\tilde{X}_I}{X_I}\right)(\kappa_L X_L + \phi X_T - e_2 X_I) \\ &+ B\left(1 - \frac{\tilde{X}_T}{X_T}\right)(\kappa_I X_I - e_4 X_T) + C\left(1 - \frac{\tilde{X}_P}{X_P}\right)(\alpha X_I - \omega X_P). \end{aligned} \tag{25}$$

Furthermore, the endemic equilibrium $\mathcal{T}^* = (\tilde{X}_S, \tilde{X}_L, \tilde{X}_I, \tilde{X}_T, \tilde{X}_P)$ satisfies

$$\begin{cases} \Pi = (\lambda_I \tilde{X}_I + \lambda_T \tilde{X}_T + \lambda_P \tilde{X}_P)\tilde{X}_S + \mu_S \tilde{X}_S, \\ e_1 \tilde{X}_L = (\lambda_I \tilde{X}_I + \lambda_T \tilde{X}_T + \lambda_P \tilde{X}_P)\tilde{X}_S, \\ e_2 \tilde{X}_I = \kappa_L \tilde{X}_L + \phi \tilde{X}_T, \\ e_4 \tilde{X}_T = \kappa_I \tilde{X}_I, \\ \omega \tilde{X}_P = \alpha \tilde{X}_I. \end{cases} \tag{26}$$

Substituting the conditions given in (26) into the above equation and simplifying, we obtain

$$\begin{aligned}\frac{dU_1}{dt} &= -\frac{\mu_S}{X_S}(X_S - \tilde{X}_S)^2 + \lambda_I \tilde{X}_S \tilde{X}_I \left(2 - \frac{\tilde{X}_S}{X_S} - \frac{X_S}{\tilde{X}_S}\frac{X_I}{\tilde{X}_I}\frac{\tilde{X}_L}{X_L}\right) \\ &+ \lambda_T \tilde{X}_S \tilde{X}_T \left(2 - \frac{\tilde{X}_S}{X_S} - \frac{X_S}{\tilde{X}_S}\frac{X_T}{\tilde{X}_T}\frac{\tilde{X}_L}{X_L}\right) + \lambda_P \tilde{X}_S \tilde{X}_P \left(2 - \frac{\tilde{X}_S}{X_S} - \frac{X_S}{\tilde{X}_S}\frac{X_P}{\tilde{X}_P}\frac{\tilde{X}_L}{X_L}\right) \\ &+ X_I(\lambda_I \tilde{X}_S - e_2 A + \kappa_I B + \alpha C) + X_T(\lambda_T \tilde{X}_S + \phi A - e_4 B) + X_L(\kappa_L A - e_1) \\ &+ X_P(\lambda_P \tilde{X}_S - \omega C) + \kappa_L A \tilde{X}_L \left(1 - \frac{X_L}{\tilde{X}_L}\frac{\tilde{X}_I}{X_I}\right) + \phi A \tilde{X}_T \left(1 - \frac{X_T}{\tilde{X}_T}\frac{\tilde{X}_I}{X_I}\right) \\ &+ \kappa_I B \tilde{X}_I \left(1 - \frac{X_I}{\tilde{X}_I}\frac{\tilde{X}_T}{X_T}\right) + \alpha C \tilde{X}_I \left(1 - \frac{X_I}{\tilde{X}_I}\frac{\tilde{X}_P}{X_P}\right). \end{aligned} \tag{27}$$

The positive constants A, B, and C are selected so that

$$\begin{cases} \lambda_I \tilde{X}_S - e_2 A + \kappa_I B + \alpha C = 0, \\ \lambda_T \tilde{X}_S + \phi A - e_4 B = 0, \\ \kappa_L A - e_1 = 0, \\ \lambda_P \tilde{X}_S - \omega C = 0. \end{cases} \tag{28}$$

The solution of the above equations gives

$$\begin{cases} A = \dfrac{e_1}{\kappa_L}, \\ B = \dfrac{\mathfrak{R}_0 e_1 \phi + \mathrm{X}_\mathrm{S}^0 \lambda_T \kappa_L}{e_4 \kappa_L \mathfrak{R}_0}, \\ C = \dfrac{\lambda_P \mathrm{X}_\mathrm{S}^0}{\omega \mathfrak{R}_0}. \end{cases} \tag{29}$$

Hence, Equation (27) takes the form

$$\begin{aligned} \frac{dU_1}{dt} = & -\frac{\mu_S}{\mathrm{X_S}}(\mathrm{X_S} - \tilde{\mathrm{X}}_\mathrm{S})^2 + \lambda_I \tilde{\mathrm{X}}_\mathrm{S} \tilde{\mathrm{X}}_\mathrm{I} \left(2 - \frac{\tilde{\mathrm{X}}_\mathrm{S}}{\mathrm{X_S}} - \frac{\mathrm{X_S}}{\tilde{\mathrm{X}}_\mathrm{S}} \frac{\mathrm{X_I}}{\tilde{\mathrm{X}}_\mathrm{I}} \frac{\tilde{\mathrm{X}}_\mathrm{L}}{\mathrm{X_L}}\right) \\ & + \lambda_T \tilde{\mathrm{X}}_\mathrm{S} \tilde{\mathrm{X}}_\mathrm{T} \left(2 - \frac{\tilde{\mathrm{X}}_\mathrm{S}}{\mathrm{X_S}} - \frac{\mathrm{X_S}}{\tilde{\mathrm{X}}_\mathrm{S}} \frac{\mathrm{X_T}}{\tilde{\mathrm{X}}_\mathrm{T}} \frac{\tilde{\mathrm{X}}_\mathrm{L}}{\mathrm{X_L}}\right) + \lambda_P \tilde{\mathrm{X}}_\mathrm{S} \tilde{\mathrm{X}}_\mathrm{P} \left(2 - \frac{\tilde{\mathrm{X}}_\mathrm{S}}{\mathrm{X_S}} - \frac{\mathrm{X_S}}{\tilde{\mathrm{X}}_\mathrm{S}} \frac{\mathrm{X_P}}{\tilde{\mathrm{X}}_\mathrm{P}} \frac{\tilde{\mathrm{X}}_\mathrm{L}}{\mathrm{X_L}}\right) \\ & + A\kappa_L \tilde{\mathrm{X}}_\mathrm{L} \left(1 - \frac{\tilde{\mathrm{X}}_\mathrm{I}}{\mathrm{X_I}} \frac{\mathrm{X_L}}{\tilde{\mathrm{X}}_\mathrm{L}}\right) + A\phi \tilde{\mathrm{X}}_\mathrm{T} \left(1 - \frac{\mathrm{X_T}}{\tilde{\mathrm{X}}_\mathrm{T}} \frac{\tilde{\mathrm{X}}_\mathrm{I}}{\mathrm{X_I}}\right) \\ & + B\kappa_I \tilde{\mathrm{X}}_\mathrm{I} \left(1 - \frac{\mathrm{X_I}}{\tilde{\mathrm{X}}_\mathrm{I}} \frac{\tilde{\mathrm{X}}_\mathrm{T}}{\mathrm{X_T}}\right) + C\alpha \tilde{\mathrm{X}}_\mathrm{I} \left(1 - \frac{\mathrm{X_I}}{\tilde{\mathrm{X}}_\mathrm{I}} \frac{\tilde{\mathrm{X}}_\mathrm{P}}{\mathrm{X_P}}\right). \end{aligned} \tag{30}$$

Using the equations in (26) together with those in (28), we obtain

$$\begin{aligned} \frac{dU_1}{dt} = & -\frac{\mu_S}{\mathrm{X_S}}(\mathrm{X_S} - \tilde{\mathrm{X}}_\mathrm{S})^2 + \lambda_I \tilde{\mathrm{X}}_\mathrm{S} \tilde{\mathrm{X}}_\mathrm{I} \left(3 - \frac{\tilde{\mathrm{X}}_\mathrm{S}}{\mathrm{X_S}} - \frac{\mathrm{X_S}}{\tilde{\mathrm{X}}_\mathrm{S}} \frac{\mathrm{X_I}}{\tilde{\mathrm{X}}_\mathrm{I}} \frac{\tilde{\mathrm{X}}_\mathrm{L}}{\mathrm{X_L}} - \frac{\mathrm{X_L}}{\tilde{\mathrm{X}}_\mathrm{L}} \frac{\tilde{\mathrm{X}}_\mathrm{I}}{\mathrm{X_I}}\right) \\ & + \lambda_T \tilde{\mathrm{X}}_\mathrm{S} \tilde{\mathrm{X}}_\mathrm{T} \left(4 - \frac{\tilde{\mathrm{X}}_\mathrm{S}}{\mathrm{X_S}} - \frac{\mathrm{X_S}}{\tilde{\mathrm{X}}_\mathrm{S}} \frac{\mathrm{X_T}}{\tilde{\mathrm{X}}_\mathrm{T}} \frac{\tilde{\mathrm{X}}_\mathrm{L}}{\mathrm{X_L}} - \frac{\tilde{\mathrm{X}}_\mathrm{T}}{\mathrm{X_T}} \frac{\mathrm{X_I}}{\tilde{\mathrm{X}}_\mathrm{I}} - \frac{\mathrm{X_L}}{\tilde{\mathrm{X}}_\mathrm{L}} \frac{\tilde{\mathrm{X}}_\mathrm{I}}{\mathrm{X_I}}\right) \\ & + \lambda_P \tilde{\mathrm{X}}_\mathrm{S} \tilde{\mathrm{X}}_\mathrm{P} \left(4 - \frac{\tilde{\mathrm{X}}_\mathrm{S}}{\mathrm{X_S}} - \frac{\mathrm{X_S}}{\tilde{\mathrm{X}}_\mathrm{S}} \frac{\mathrm{X_P}}{\tilde{\mathrm{X}}_\mathrm{P}} \frac{\tilde{\mathrm{X}}_\mathrm{L}}{\mathrm{X_L}} - \frac{\tilde{\mathrm{X}}_\mathrm{P}}{\mathrm{X_P}} \frac{\mathrm{X_I}}{\tilde{\mathrm{X}}_\mathrm{I}} - \frac{\mathrm{X_L}}{\tilde{\mathrm{X}}_\mathrm{L}} \frac{\tilde{\mathrm{X}}_\mathrm{I}}{\mathrm{X_I}}\right) \\ & + A\phi \tilde{\mathrm{X}}_\mathrm{T} \left(2 - \frac{\mathrm{X_T}}{\tilde{\mathrm{X}}_\mathrm{T}} \frac{\tilde{\mathrm{X}}_\mathrm{I}}{\mathrm{X_I}} - \frac{\tilde{\mathrm{X}}_\mathrm{T}}{\mathrm{X_T}} \frac{\mathrm{X}_I}{\tilde{\mathrm{X}}_\mathrm{I}}\right). \end{aligned} \tag{31}$$

Since $\mathfrak{R}_0 > 1$, the endemic-equilibrium components satisfy $\tilde{\mathrm{X}}_\mathrm{S}, \tilde{\mathrm{X}}_\mathrm{L}, \tilde{\mathrm{X}}_\mathrm{I}, \tilde{\mathrm{X}}_\mathrm{T}, \tilde{\mathrm{X}}_\mathrm{P} > 0$. We now verify the non-positivity of the bracketed expressions in Equation (31) using the arithmetic–geometric mean inequality. Consider first the bracket containing three ratios. Let

$$u_1 = \frac{\tilde{\mathrm{X}}_\mathrm{S}}{\mathrm{X_S}}, \qquad u_2 = \frac{\mathrm{X_S X_I} \tilde{\mathrm{X}}_\mathrm{L}}{\tilde{\mathrm{X}}_\mathrm{S} \tilde{\mathrm{X}}_\mathrm{I} \mathrm{X_L}}, \qquad u_3 = \frac{\mathrm{X_L} \tilde{\mathrm{X}}_\mathrm{I}}{\tilde{\mathrm{X}}_\mathrm{L} \mathrm{X_I}}.$$

The product of these three positive quantities is

$$u_1 u_2 u_3 = \frac{\tilde{\mathrm{X}}_\mathrm{S}}{\mathrm{X_S}} \frac{\mathrm{X_S X_I} \tilde{\mathrm{X}}_\mathrm{L}}{\tilde{\mathrm{X}}_\mathrm{S} \tilde{\mathrm{X}}_\mathrm{I} \mathrm{X_L}} \frac{\mathrm{X_L} \tilde{\mathrm{X}}_\mathrm{I}}{\tilde{\mathrm{X}}_\mathrm{L} \mathrm{X_I}} = 1.$$

Therefore, by the arithmetic–geometric mean inequality,

$$u_1 + u_2 + u_3 \geq 3\sqrt[3]{u_1 u_2 u_3} = 3,$$

which implies that

$$3 - u_1 - u_2 - u_3 \leq 0.$$

Similarly, since the product of the positive ratios in each of the remaining bracketed expressions is equal to one, the arithmetic–geometric mean inequality gives

$$4 - \frac{\tilde{\mathrm{X}}_\mathrm{S}}{\mathrm{X_S}} - \frac{\mathrm{X_S X_T} \tilde{\mathrm{X}}_\mathrm{L}}{\tilde{\mathrm{X}}_\mathrm{S} \tilde{\mathrm{X}}_\mathrm{T} \mathrm{X_L}} - \frac{\tilde{\mathrm{X}}_\mathrm{T} \mathrm{X_I}}{\mathrm{X_T} \tilde{\mathrm{X}}_\mathrm{I}} - \frac{\mathrm{X_L} \tilde{\mathrm{X}}_\mathrm{I}}{\tilde{\mathrm{X}}_\mathrm{L} \mathrm{X_I}} \leq 0,$$

$$4 - \frac{\tilde{X}_S}{X_S} - \frac{X_S X_P \tilde{X}_L}{\tilde{X}_S \tilde{X}_P X_L} - \frac{\tilde{X}_P X_I}{X_P \tilde{X}_I} - \frac{X_L \tilde{X}_I}{\tilde{X}_L X_I} \leq 0,$$

and

$$2 - \frac{X_T \tilde{X}_I}{\tilde{X}_T X_I} - \frac{\tilde{X}_T X_I}{X_T \tilde{X}_I} \leq 0.$$

Hence, all the bracketed expressions in Equation (31) are non-positive. Since their coefficients are positive, it follows that $\frac{dU_1}{dt} \leq 0, \forall X_S, X_L, X_I, X_T, X_P > 0$. Hence, U_1 is a Lyapunov function for the system of equations governing the state variables X_S, X_L, X_I, X_T, and X_P in model (1). From Equation (31), $\frac{dU_1}{dt} = 0$ requires $X_S = \tilde{X}_S$. Moreover, equality in the arithmetic–geometric mean inequalities requires a common ratio, denoted by

$$r = \frac{X_L}{\tilde{X}_L} = \frac{X_I}{\tilde{X}_I} = \frac{X_T}{\tilde{X}_T} = \frac{X_P}{\tilde{X}_P}.$$

Thus,

$$X_I = r\tilde{X}_I, \qquad X_T = r\tilde{X}_T, \qquad X_P = r\tilde{X}_P.$$

For a solution to remain in the equality set, we must have $X_S = \tilde{X}_S$ and $\dot{X}_S = 0$. Hence, the susceptible equation becomes

$$0 = \Pi - r\left(\lambda_I \tilde{X}_I + \lambda_T \tilde{X}_T + \lambda_P \tilde{X}_P\right)\tilde{X}_S - \mu_S \tilde{X}_S. \tag{32}$$

On the other hand, the susceptible equilibrium relation in Equation (4a) is

$$0 = \Pi - \left(\lambda_I \tilde{X}_I + \lambda_T \tilde{X}_T + \lambda_P \tilde{X}_P\right)\tilde{X}_S - \mu_S \tilde{X}_S. \tag{33}$$

Subtract Equation (33) from Equation (32) gives

$$(1 - r)\left(\lambda_I \tilde{X}_I + \lambda_T \tilde{X}_T + \lambda_P \tilde{X}_P\right)\tilde{X}_S = 0.$$

Since

$$\left(\lambda_I \tilde{X}_I + \lambda_T \tilde{X}_T + \lambda_P \tilde{X}_P\right)\tilde{X}_S > 0,$$

when $\mathfrak{R}_0 > 1$, we obtain $1 - r = 0$, and therefore $r = 1$. Consequently,

$$X_S = \tilde{X}_S, \quad X_L = \tilde{X}_L, \quad X_I = \tilde{X}_I, \quad X_T = \tilde{X}_T, \quad \text{and} \quad X_P = \tilde{X}_P.$$

Thus, the largest invariant subset of $\left\{\frac{dU_1}{dt} = 0\right\}$ is $\{(\tilde{X}_S, \tilde{X}_L, \tilde{X}_I, \tilde{X}_T, \tilde{X}_P)\}$. Therefore, LaSalle's Invariance Principle [24] implies that

$$(X_S, X_L, X_I, X_T, X_P) \longrightarrow (\tilde{X}_S, \tilde{X}_L, \tilde{X}_I, \tilde{X}_T, \tilde{X}_P) \quad \text{as } t \to \infty.$$

It follows that $\lim_{t\to\infty} X_L = \tilde{X}_L$. Thus, for every sufficiently small $\varepsilon_T > 0$, there exists a $N_1 > 0$ such that $X_L \leq \tilde{X}_L + \varepsilon_T, \forall\, t > N_1$. From model (1)'s fourth equation, for $t > N_1$ we have

$$\dot{X_Q} = q_L X_L - e_3 X_Q \leq q_L(\tilde{X}_L + \varepsilon_T) - e_3 X_Q.$$

Therefore, by the Comparison Theorem [25],

$$X_Q^{\infty} = \limsup_{t\to\infty} X_Q \leq \frac{q_L(\tilde{X}_L + \varepsilon_T)}{e_3}.$$

Letting $\varepsilon_T \to 0$, we obtain

$$X_Q^{\infty} = \limsup_{t\to\infty} X_Q \leq \frac{q_L \tilde{X}_L}{e_3} = \tilde{X}_Q.$$

Similarly, using $\liminf_{t\to\infty} X_L = \tilde{X}_L$, it follows that

$$X_{Q_\infty} = \liminf_{t\to\infty} X_Q \geq \frac{q_L \tilde{X}_L}{e_3} = \tilde{X}_Q.$$

Consequently,

$$X_{Q_\infty} \geq \tilde{X}_Q \geq X_Q^{\infty}.$$

Therefore, $\lim_{t\to\infty} X_Q = \tilde{X}_Q$. By the same argument, we can show that $\lim_{t\to\infty} X_R = \tilde{X}_R$. Hence, as $t \to \infty$

$$(X_S, X_L, X_I, X_Q, X_T, X_P, X_R) \longrightarrow (\tilde{X}_S, \tilde{X}_L, \tilde{X}_I, \tilde{X}_Q, \tilde{X}_T, \tilde{X}_P, \tilde{X}_R).$$

Consequently, for $\mathfrak{R}_0 > 1$, all solutions of model (1) with initial conditions in Ω_T° converge to $\mathcal{T}^*$ as $t \to \infty$. Hence, whenever $\mathfrak{R}_0 > 1$, the endemic equilibrium $\mathcal{T}^*$ is globally asymptotically stable in Ω_T°. □

4. Sensitivity and Threshold Analysis

4.1. Local Sensitivity Analysis

Analysis of local sensitivity is a crucial method for computing the factors that have the most impact on the spread of the illness and for directing successful TB control measures. We may measure each parameter's proportionate contribution to the disease's spread by assessing the sensitivity of the basic reproduction number ($\mathfrak{R}_0$) with regard to the model parameters. In order to plan and optimize control strategies, including vaccines, early identification, treatment, and environmental interventions, we assess the sensitivity of $\mathfrak{R}_0$ to each model's parameter with the normalized sensitivity index. In relation to a parameter (ν), the normalization sensitivity index of ($\mathfrak{R}_0$) is defined as follows:

$$\Theta_{\nu}^{\mathfrak{R}_0} = \frac{\partial \mathfrak{R}_0}{\partial \nu} \times \frac{\nu}{\mathfrak{R}_0}. \tag{34}$$

We can thus determine the effect of changing each parameter on $\mathfrak{R}_0$ by utilizing the formula (34) to calculate all partial derivatives of the parameters with regard to $\mathfrak{R}_0$. For example, a positive sensitivity index indicates that increasing the relevant parameter increases the critical reproduction number, $\mathfrak{R}_0$, whereas a negative index indicates that increasing the parameter decreases $\mathfrak{R}_0$. The effect of parameters on $\mathfrak{R}_0$ is shown in Table 3 and, for clarity, these values are specified in the flowchart (see Figure 2). Based on the sensitivity analysis presented in Table 3, the largest effects on the $\mathfrak{R}_0$ are associated with the recruitment rate Π, with sensitivity index $\Theta_{\Pi}^{\mathfrak{R}_0} = +1$, and the mortality rate of susceptible individuals μ_S, with sensitivity index $\Theta_{\mu_S}^{\mathfrak{R}_0} = -1$. This implies that a 10% increase in μ_S reduces $\mathfrak{R}_0$ by 10%, whereas a 10% increase (or decrease) in Π increases (or decreases) $\mathfrak{R}_0$ by 10%. However, μ_S is a demographic parameter and should not be interpreted as a practical intervention target. Among the TB-related parameters, the environmental pathogen-clearance rate ω has the largest negative sensitivity index, $\Theta_{\omega}^{\mathfrak{R}_0} = -0.77$. Thus, measures that enhance the removal or inactivation of viable *Mycobacterium tuberculosis* from the air, such as improved ventilation and ultraviolet germicidal irradiation, may substantially reduce disease transmission [3,26]. The sensitivity indices for the preventive-treatment initiation rate, q_L, and the treatment initiation rate, κ_I, are quite large and negative, with $\Theta_{q_L}^{\mathfrak{R}_0} = -0.68$ and

$\Theta_{\kappa_I}^{\mathfrak{R}_0} = -0.58$, respectively. Therefore, a 10% increase in q_L or κ_I reduces $\mathfrak{R}_0$ by approximately 6.8% or 5.8%, respectively. These findings demonstrate the importance of expanding preventive treatment among latently infected individuals and ensuring timely treatment initiation among infectious individuals. The mortality rate of infectious individuals, μ_I, has a negative sensitivity index, $\Theta_{\mu_I}^{\mathfrak{R}_0} = -0.41$. In contrast, the MTB shedding rate α and the environmental transmission coefficient λ_P have comparatively large positive sensitivity indices, with $\Theta_{\alpha}^{\mathfrak{R}_0} = +0.78$ and $\Theta_{\lambda_P}^{\mathfrak{R}_0} = +0.77$, respectively. In this observation we stress the role of the environmental route in maintaining TB transmission and the need for proper ventilation, airborne infection control measures, and approaches to lower the concentration of viable *Mycobacterium tuberculosis* in the environment. The progression rate from latent infection to active infectious tuberculosis, κ_L, also has a relatively large positive sensitivity index, $\Theta_{\kappa_L}^{\mathfrak{R}_0} = +0.71$. The direct transmission coefficient, λ_I, has a moderate positive sensitivity index, $\Theta_{\lambda_I}^{\mathfrak{R}_0} = +0.23$. Finally, the treatment failure rate, ϕ, has a comparatively small positive sensitivity index, $\Theta_{\phi}^{\mathfrak{R}_0} = +0.06$. Although this local effect is relatively small, treatment failure remains epidemiologically important because it returns individuals undergoing treatment to the infectious class. Overall, effective control of TB transmission requires a comprehensive strategy that combines reductions in direct and environmental transmission, prevention of progression from latent infection to active tuberculosis, expansion of preventive treatment, timely initiation of active-TB treatment, reduction of treatment failure, and improved clearance of the environmental pathogen burden.

Table 3. The basic reproduction number $\mathfrak{R}_0$'s normalized forward sensitivity indices in relation to the model (1). The sensitivity indices were computed using the baseline parameter values listed in Table 2.

Parameter	Π	λ_I	κ_L	λ_P	α	ϕ	η	-
Sensitivity index	1.00	0.23	0.71	0.77	0.78	0.06	0.005	-
Parameter	μ_S	μ_I	ω	κ_I	q_L	μ_L	μ_T	γ_T
Sensitivity index	−1.00	−0.41	−0.77	−0.58	−0.68	−0.03	−0.002	−0.06

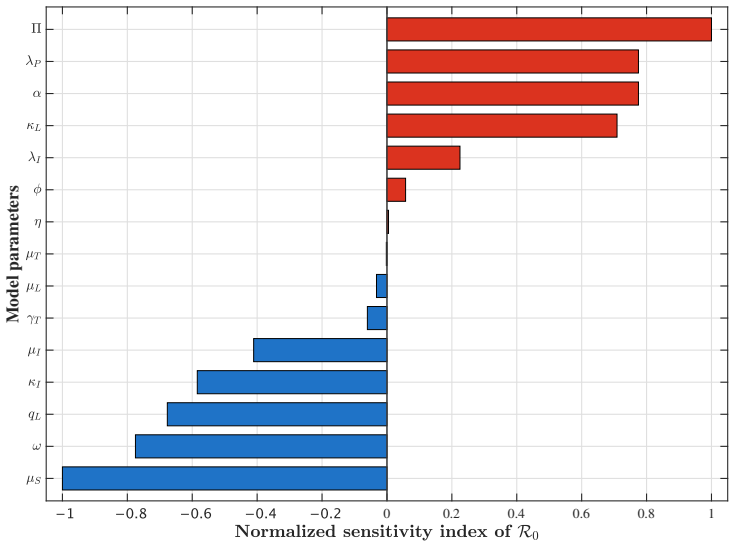


Figure 2. Bar graph showing the normalized forward sensitivity indices of $\mathfrak{R}_0$ with respect to the parameters of model (1). Red bars indicate positive sensitivity: increasing the corresponding parameter increases $\mathfrak{R}_0$. Blue bars indicate negative sensitivity: increasing the corresponding parameter decreases $\mathfrak{R}_0$. Larger absolute indices indicate greater local sensitivity. For the baseline parameter values used here, the indices range from -1 to $+1$, with Π and μ_S having the largest absolute indices.

Furthermore, Figure 3 illustrates the combined effects of selected parameter pairs on $\mathfrak{R}_0$, while all other parameters are fixed at their baseline values. The transition from blue to red represents an increase in $\mathfrak{R}_0$. In panels (a), (b), and (d), $\mathfrak{R}_0$ increases with the direct and environmental transmission coefficients (λ_I, λ_P), the recruitment and treatment failure rates (Π, ϕ), and the progression and MTB shedding rates (κ_L, α), respectively. These relationships demonstrate that direct transmission, environmental exposure, treatment failure, progression to active TB, and pathogen shedding promote disease transmission. Conversely, panels (c), (e), and (f) show that $\mathfrak{R}_0$ decreases with increasing latent mortality and environmental pathogen-clearance rates (μ_L, ω), the preventive-treatment initiation and infectious mortality rates (q_L, μ_I), and the susceptible mortality and treatment initiation rates (μ_S, κ_I), respectively. In particular, increasing ω reduces the persistence of viable *Mycobacterium tuberculosis* in the environment, increasing q_L limits progression to active TB, and increasing κ_I shortens the duration of untreated infectiousness. Although μ_S, μ_L, and μ_I have negative mathematical effects on $\mathfrak{R}_0$, mortality is not considered a practical intervention mechanism. Overall, the response surfaces are consistent with the normalized local sensitivity indices reported in Table 3 and Figure 2.

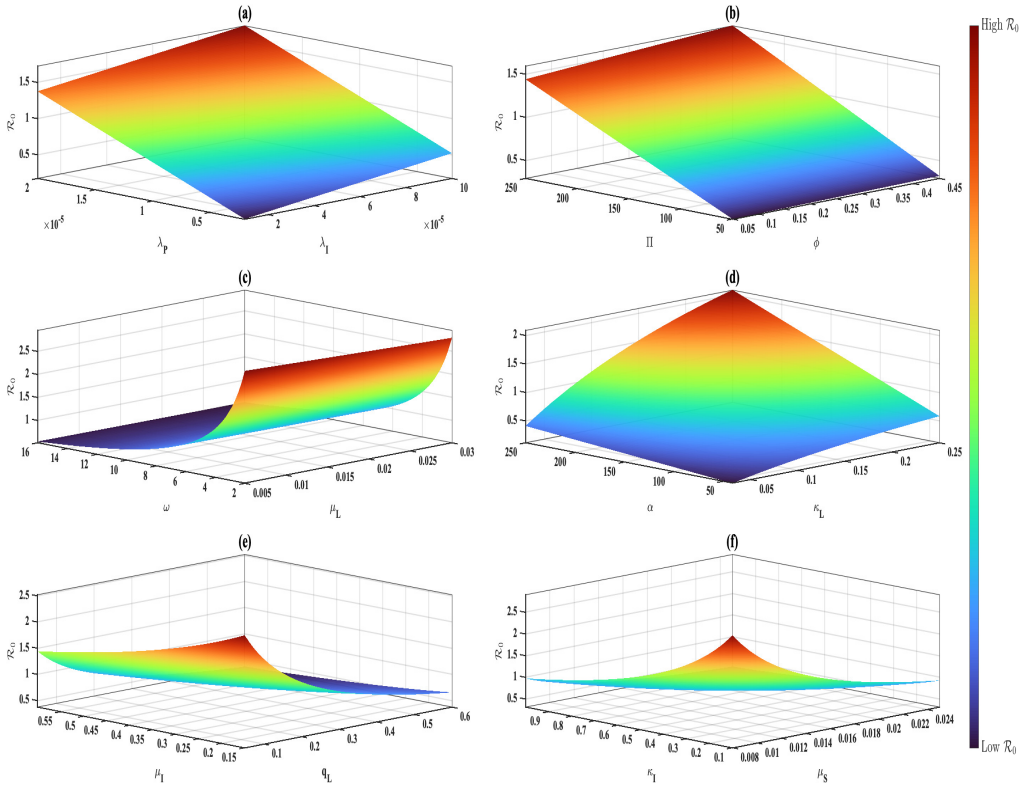


Figure 3. The influence of altering modeling parameters on $\mathfrak{R}_0$: (**a**) $\mathfrak{R}_0$ compared to λ_I and λ_P; (**b**) $\mathfrak{R}_0$ compared to ϕ and Π; (**c**) $\mathfrak{R}_0$ compared to μ_L and ω; (**d**) $\mathfrak{R}_0$ compared to κ_L and α; (**e**) $\mathfrak{R}_0$ compared to q_L and μ_I; (**f**) $\mathfrak{R}_0$ compared to μ_S and κ_I. Blue and red regions represent lower and higher values of $\mathfrak{R}_0$, respectively.

4.2. Global Sensitivity Analysis

The global sensitivity analysis examines the impact of simultaneous variations of the model parameters within their prescribed ranges. In contrast, local sensitivity analysis studies the effect of varying one parameter around the baseline point while holding the other parameters constant. In this subsection, we used the Latin hypercube sampling (LHS) and partial rank correlation coefficients (PRCCs) to assess parameter uncertainty and to identify the parameters that have the strongest influence on the basic reproduction number $\mathfrak{R}_0$ [27]. A total of 5000 parameter sets were generated, and $\mathfrak{R}_0$ was calculated for each set. Positive

and negative PRCC values indicate positive and negative monotonic associations with $\mathfrak{R}_0$, respectively, while $p < 0.05$ indicates statistical significance. The baseline value was $\mathfrak{R}_0 = 0.864$. Across the sampled parameter sets, $\mathfrak{R}_0$ ranged from 0.371 to 2.059, with 70.60% of the sampled values satisfying $\mathfrak{R}_0 < 1$ and 29.40% satisfying $\mathfrak{R}_0 > 1$. Thus, parameter uncertainty may shift the system from the elimination region to the persistence region. The results of PRCC are presented in Table 4 and Figure 4. As shown in Table 4 and Figure 4, Π has the strongest positive association with $\mathfrak{R}_0$ (PRCC = 0.9000), followed by α (0.8470), λ_P (0.8438), and κ_L (0.8219). The effects of λ_I (0.4120) and ϕ (0.1257) are positive but less strong. Conversely, μ_S has the strongest negative association (-0.8986), followed by ω (-0.8432), q_L (-0.8061), κ_I (-0.7626), and μ_I (-0.6446). The findings emphasize the significance of the environmental transmission route and indicate a large decrease in transmission with better pathogen elimination, preventive measures, and early start of active-TB therapy. Although γ_T and μ_L exhibit weak but statistically significant negative associations with $\mathfrak{R}_0$, the associations of μ_T and η with $\mathfrak{R}_0$ are not statistically significant because their p-values exceed 0.05. Overall, the PRCC results are consistent with the local sensitivity indices in Table 3 and support interventions targeting direct and environmental transmission, pathogen shedding, preventive treatment, treatment initiation, and treatment failure.

Table 4. Partial rank correlation coefficients (PRCCs) and corresponding p-values of the $\mathfrak{R}_0$ with respect to the parameters of model (1). The PRCC values were computed using 5000 parameter sets generated by Latin hypercube sampling over the prescribed parameter ranges.

Parameter	Π	λ_I	κ_L	λ_P	α	ϕ	η	–
PRCC	0.9000	0.4120	0.8219	0.8438	0.8470	0.1257	0.0106	–
p-value	< 0.001	< 0.001	< 0.001	< 0.001	< 0.001	< 0.001	0.4556	–
Parameter	μ_S	μ_I	ω	κ_I	q_L	μ_L	μ_T	γ_T
PRCC	-0.8986	-0.6446	-0.8432	-0.7626	-0.8061	-0.0851	-0.0121	-0.1216
p-value	< 0.001	< 0.001	< 0.001	< 0.001	< 0.001	< 0.001	0.3928	< 0.001

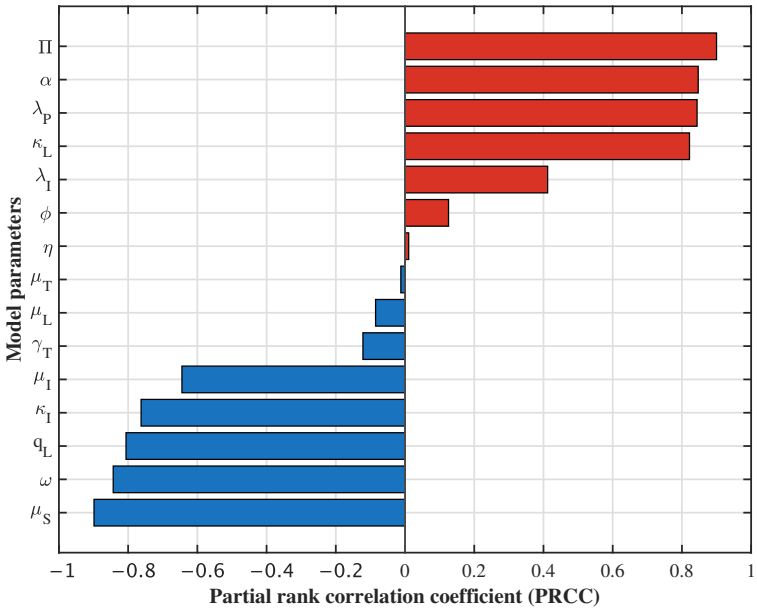


Figure 4. Partial rank correlation coefficients (PRCCs) between the model parameters and the basic reproduction number $\mathfrak{R}_0$, calculated from 5000 Latin hypercube samples. Positive PRCC values (**red**) indicate that increasing the corresponding parameter tends to increase $\mathfrak{R}_0$, whereas negative values (**blue**) indicate an inverse relationship. Larger absolute PRCC values represent stronger global parameter influence.

4.3. Threshold Analysis in the (ϕ, η)-Plane

Although local and global sensitivity analyses quantify the individual influence of model parameters on $\mathfrak{R}_0$, they do not identify combinations of parameter values that maintain $\mathfrak{R}_0 < 1$. Both analyses indicate that ϕ has a weak positive influence on $\mathfrak{R}_0$, whereas the influence of η is negligible at the adopted baseline values and over the prescribed parameter ranges. Nevertheless, ϕ and η were selected for the threshold analysis because they represent two complementary treatment-related mechanisms that are central to the model. The parameter ϕ governs the return of treated individuals to the infectious class, whereas η measures their residual infectiousness during treatment. Examining these parameters jointly therefore reveals whether sufficiently low residual infectiousness can offset the adverse effect of increased treatment failure and maintain $\mathfrak{R}_0 < 1$, a relationship that cannot be identified from their individual sensitivity measures alone. Thus, we undertake a threshold analysis in the (ϕ, η)-plane to examine their combined effect. The biologically viable parameter space is divided into TB-elimination ($\mathcal{R}_0 < 1$) and TB-persistence ($\mathcal{R}_0 > 1$) areas by solving the threshold equation $\mathcal{R}_0 = 1$, which yields the key connection between ϕ and η. Since the relative infectiousness of treated individuals satisfies

$$0 < \eta < 1.$$

We solve the threshold equation with respect to η to get its critical value, the $\mathfrak{R}_0$ can be rewritten in terms of λ_I, using the relation $\lambda_T = \eta\lambda_I$, as follows:

$$\mathfrak{R}_0 = \frac{\kappa_L \mathrm{X}_\mathrm{S}^0(\lambda_I \omega e_4 + \lambda_I \eta \omega \kappa_I + \alpha \lambda_P e_4)}{\omega e_1(e_2 e_4 - \kappa_I \phi)},$$

where e_1, e_2, e_3, and e_4 are defined in (5). Let

$$M = \gamma_T + \mu_T, \qquad Z = \alpha\lambda_P + \lambda_I \omega,$$

so that

$$e_4 = \phi + M.$$

The basic reproduction number can therefore be expressed as

$$\mathfrak{R}_0 = \frac{\mathrm{X}_\mathrm{S}^0 \kappa_L((\phi + M)Z + \lambda_I \eta \kappa_I \omega)}{e_1 \omega((\phi + M)e_2 - \kappa_I \phi)}.$$

Solving $\mathfrak{R}_0 = 1$ for η yields the critical value of η^* as a function of ϕ, which gives

$$\eta^*(\phi) = \frac{e_1 \omega(e_2 M + \phi \mu_I) - \mathrm{X}_\mathrm{S}^0 \kappa_L(\phi + M)Z}{\mathrm{X}_\mathrm{S}^0 \kappa_L \lambda_I \kappa_I \omega}.$$

Therefore, the TB disease can be controlled whenever

$$0 < \eta < \eta^*(\phi),$$

provided that $0 < \eta^*(\phi) < 1$. Therefore, for a particular treatment-failure rate, $\eta^*(\phi)$ indicates the highest acceptable relative infectiousness of treated persons needed to avoid prolonged TB transmission. If the infectiousness of treated individuals is greater than this critical level, medication alone is inadequate to stop the transmission of tuberculosis. Hence, the threshold value $\eta^*(\phi)$ partitions the biologically feasible parameter space as follows:

$$\begin{cases} \mathfrak{R}_0 < 1, & \text{if } 0 < \eta < \eta^*(\phi), \\ \mathfrak{R}_0 = 1, & \text{if } \eta = \eta^*(\phi), \\ \mathfrak{R}_0 > 1, & \text{if } \eta > \eta^*(\phi). \end{cases}$$

Figure 5 illustrates the threshold connection in the (ϕ, η)-plane to further explore the combined impact of treatment failure and the residual infectiousness of treated persons. The threshold curve $\eta = \eta^*(\phi)$ (or equivalently $\mathfrak{R}_0 = 1$) separates the biologically feasible parameter space into two different regions. The area below the threshold curve represents the set of parameter combinations for which $\mathfrak{R}_0 < 1$, implying that, on average, each infectious individual causes less than one secondary infection, and the disease will eventually be eliminated. In contrast, the area above the threshold curve, or $\mathfrak{R}_0 > 1$, is the state where the population continues spreading across the population. Figure 5 further illustrates the trade-off between the relative infectiousness of treated individuals, η, and the treatment-failure rate, ϕ. As ϕ increases, the range of values of η for which $\mathfrak{R}_0 < 1$ becomes progressively narrower. Therefore, higher treatment-failure rates require substantially lower infectiousness among treated individuals to maintain $\mathfrak{R}_0 < 1$ and prevent sustained TB transmission. The analytical threshold obtained in this subsection is numerically verified in Section 5.2 using the same fixed parameter values and two (ϕ, η) combinations selected from opposite sides of the threshold curve.

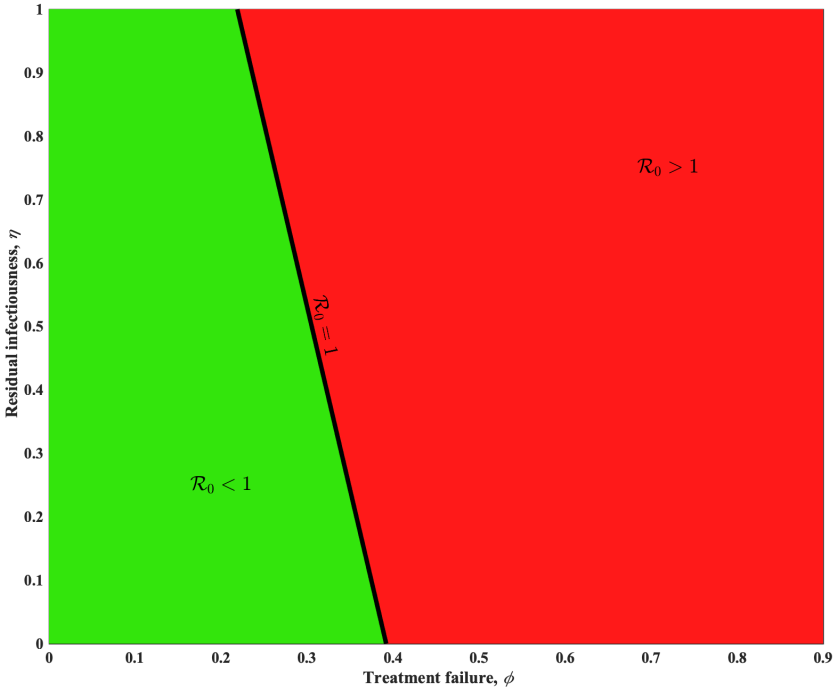


Figure 5. The (ϕ, η)-plane threshold areas. The TB-elimination region ($\mathfrak{R}_0 < 1$) and the TB-persistence region ($\mathfrak{R}_0 > 1$) are separated by the curve $\mathfrak{R}_0 = 1$, which defines the significant correlation between the treatment-failure rate (ϕ) and the relative infectiousness of treated persons (η). For this threshold illustration, only λ_P was increased to 1.15×10^{-5}, whereas all other parameter values were set to the baseline values shown in Table 2.

5. Numerical Simulations

The numerical simulations of model (1) were performed in MATLAB R2021a (version 9.10.0.1602886) using the built-in solver `ode45`, an explicit Runge–Kutta method of orders four and five with adaptive step-size control. The numerical simulations are performed to demonstrate the qualitative behavior of the model under the selected parameter

values. The model has not been calibrated or validated using data from a specific geographical setting; therefore, the results should not be interpreted as quantitative predictions or direct policy recommendations.

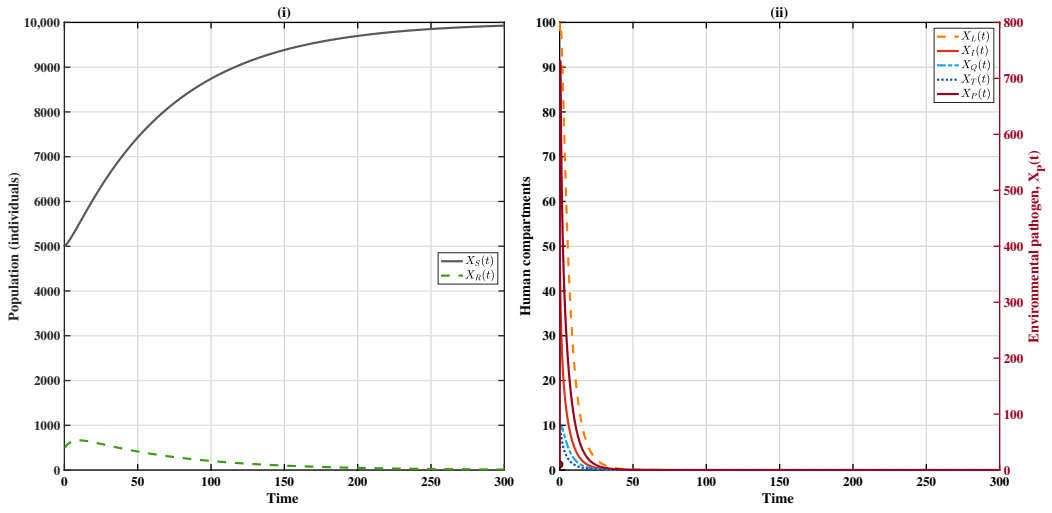
5.1. Model Dynamics

To demonstrate the suggested TB model's qualitative behavior, numerical simulations are first performed using a representative initial condition. Two scenarios are considered, corresponding to $\mathcal{R}_0 < 1$ and $\mathcal{R}_0 > 1$, while all model parameters are fixed as listed in Table 2. The resulting trajectories of state variables are presented to demonstrate the long-term dynamics of the system under the two epidemiological regimes:

Scenario 1: Dynamics under a representative initial condition.

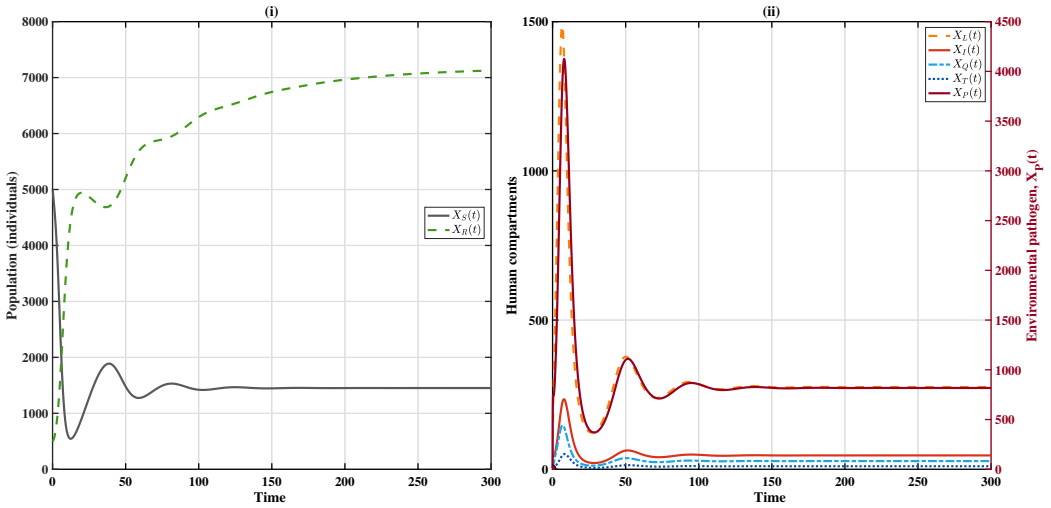
A typical starting point situation is initially used to show the qualitative dynamics of the model (1). The initial conditions are $(X_S(0), X_L(0), X_I(0), X_Q(0), X_T(0), X_P(0), X_R(0)) = (5000, 100, 50, 5, 5, 10, 500)$. The asymptotic convergence of the state variables toward the TB-free equilibrium ($\mathcal{T}_0$) and TB-endemic equilibrium ($\mathcal{T}^*$) established in Section 3.3 is demonstrated through numerical simulations for the two epidemiological regimes, $\mathfrak{R}_0 < 1$ and $\mathfrak{R}_0 > 1$. Figure 6 consists of two subpanels: (a) shows the convergence to the TB-free equilibrium ($\mathfrak{R}_0 = 0.864 < 1$), and (b) shows the convergence to the TB-endemic equilibrium ($\mathfrak{R}_0 = 6.888 > 1$). The parameters of the baseline shown in Table 2 are used here. We will choose the parameter λ_P in the following:

Case (a): $\mathfrak{R}_0 \leq 1$. Setting $\lambda_P = 1 \times 10^{-5}$, its baseline value listed in Table 2, gives $\mathfrak{R}_0 = 0.864 < 1$. Theorem 1 states that $\mathcal{T}_0$ is GAS. The theoretical and numerical results of Theorem 1 are similar, as shown in Figure 6a. The susceptible population grows and tends to its TB-free equilibrium value, $X_S^0 = \frac{\Pi}{\mu_S} = 10,000$. Meanwhile, the populations in the latent (X_L), infectious (X_I), preventive treated (X_Q), active treated (X_T), environmental pathogen (X_P), and recovered (X_R) decline over time and eventually vanish, converging to zero.
Case (b): $\mathfrak{R}_0 > 1$. Let us take $\lambda_P = 1 \times 10^{-4}$. We then obtain $\mathfrak{R}_0 = 6.888$. As shown in Figure 6b, $\mathcal{T}^*$ is GAS, and the numerical results are consistent with the theoretical results in Theorem 2. The solutions of the model (1) approach $\mathcal{T}^* = (\tilde{X}_S, \tilde{X}_L, \tilde{X}_I, \tilde{X}_Q, \tilde{X}_T, \tilde{X}_P, \tilde{X}_R) = (1451.81, 275.48, 46.45, 27.42, 10.15, 817.41, 7177.85)$.



(**a**)

Figure 6. *Cont.*



(b)

Figure 6. Dynamics of model (1) under two distinct threshold regimes. In (**a**), $\lambda_P = 1 \times 10^{-5}$ and $\mathfrak{R}_0 = 0.86 < 1$, and the trajectories converge to the TB-free equilibrium $\mathcal{T}_0$. In (**b**), $\lambda_P = 1 \times 10^{-4}$ and $\mathfrak{R}_0 = 6.88 > 1$, and the trajectories converge to the endemic equilibrium $\mathcal{T}^*$. Panels (i) show the dynamics of $X_S(t)$ and $X_R(t)$, whereas panels (ii) show the dynamics of $X_L(t)$, $X_I(t)$, $X_Q(t)$, $X_T(t)$, and $X_P(t)$. The same initial conditions are used in both cases, and all other parameter values are listed in Table 2.

Scenario 2: Dynamics under different initial conditions.

To provide numerical support for the global stability findings developed in Theorems 1 and 2, the proposed model is simulated using three different initial conditions while all parameter values are kept unchanged. The dynamics of the susceptible, latent, infectious, and environmental pathogen variables are presented for two epidemiological regimes: $\mathfrak{R}_0 = 0.864 < 1$, obtained using the baseline value $\lambda_P = 1 \times 10^{-5}$ listed in Table 2, and $\mathfrak{R}_0 = 6.888 > 1$, obtained using $\lambda_P = 1 \times 10^{-4}$. The corresponding trajectories are shown in Figure 7a–d. The following initial conditions are considered, in the order

$$IC_1 = (9340, 100, 50, 5, 5, 10, 500),$$
$$IC_2 = (8000, 500, 100, 50, 50, 25, 1300),$$
$$IC_3 = (6000, 1500, 300, 100, 100, 50, 2000).$$

Case (I): For $\mathfrak{R}_0 = 0.864 < 1$, all trajectories originating from the three initial conditions converge to the TB-free equilibrium $\mathcal{T}_0 = (10000, 0, 0, 0, 0, 0, 0)$. In particular, the susceptible population approaches its TB-free equilibrium value, whereas the latent, infectious, and environmental pathogen variables asymptotically approach zero. This numerical behavior is in agreement with the global asymptotic stability of the TB-free equilibrium proved in Theorem 1 for $\mathfrak{R}_0 \leq 1$.

Case (II): For $\mathfrak{R}_0 = 6.888 > 1$, trajectories originating from the three different initial conditions converge to the same positive endemic equilibrium. In particular, the susceptible, latent, infectious, and environmental pathogen variables approach their corresponding endemic equilibrium values. The convergence of the trajectories toward the same endemic state, independently of the selected initial conditions, provides numerical support for the global asymptotic stability result established in Theorem 2. Overall, these simulations illustrate that the long-term behavior of model (1) is governed by the basic reproduction number $\mathfrak{R}_0$: the disease is eliminated when $\mathfrak{R}_0 < 1$ and persists at an endemic level when $\mathfrak{R}_0 > 1$. Thus, the numerical results are consistent with the theoretical global stability analysis.

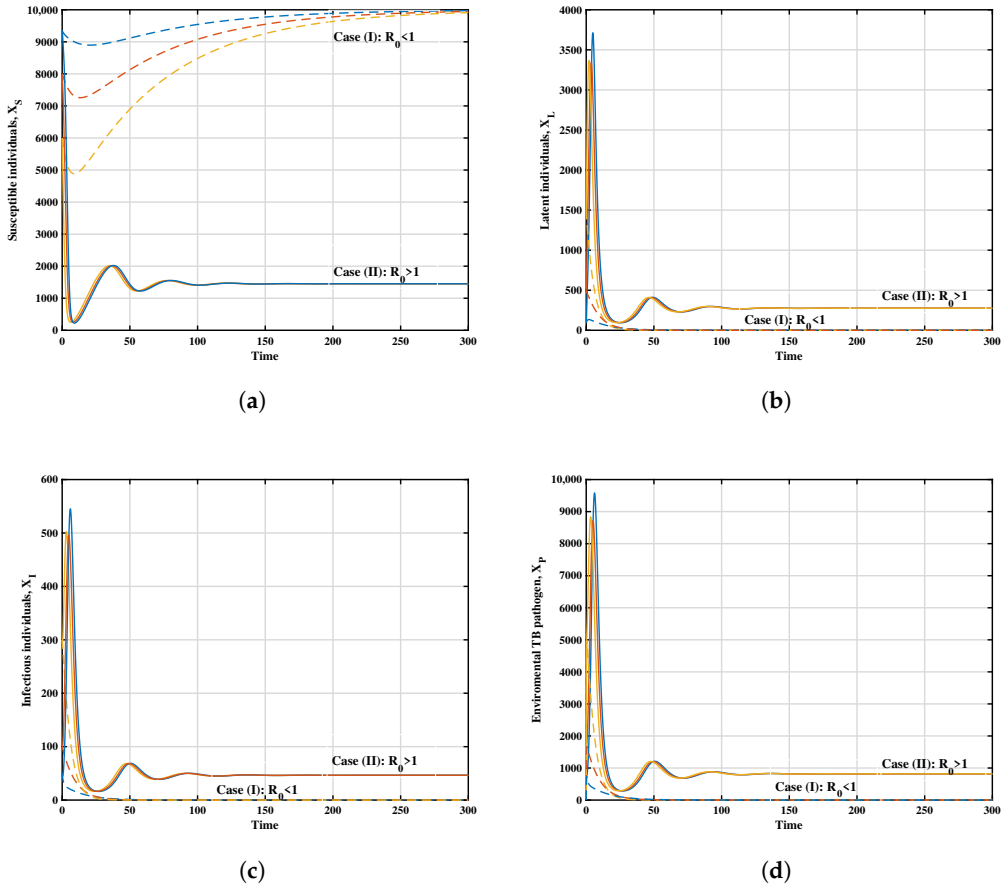
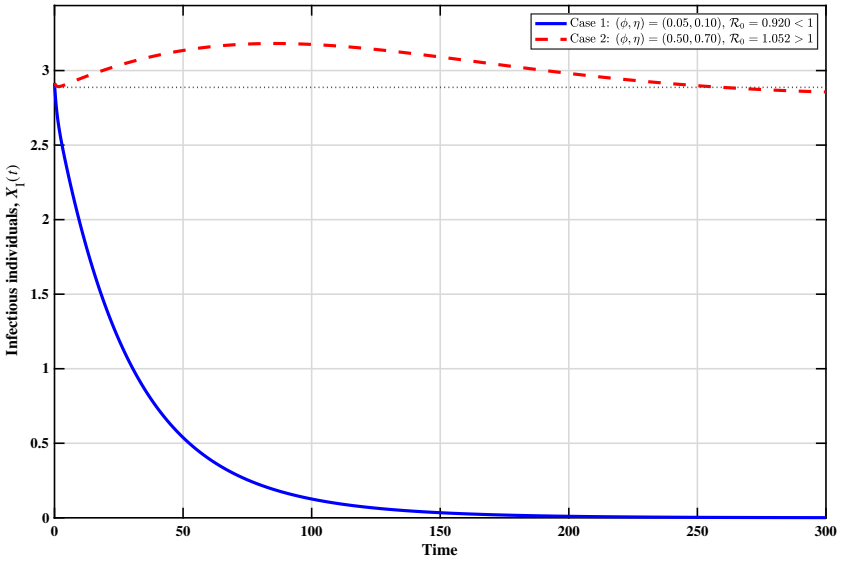


Figure 7. Numerical illustration of the global stability results using three different initial conditions. Panels (**a**–**d**) show the dynamics of the susceptible population $X_S(t)$, latent population $X_L(t)$, infectious population $X_I(t)$, and environmental pathogen concentration $X_P(t)$, respectively. Case (I), represented by dashed curves, corresponds to the TB-free regime with $\Re_0 = 0.864 < 1$, whereas Case (II), represented by solid curves, corresponds to the endemic regime with $\Re_0 = 6.888 > 1$. The blue, red, and orange curves correspond to the first, second, and third initial conditions specified in the text, respectively. All other parameter values are listed in Table 2.

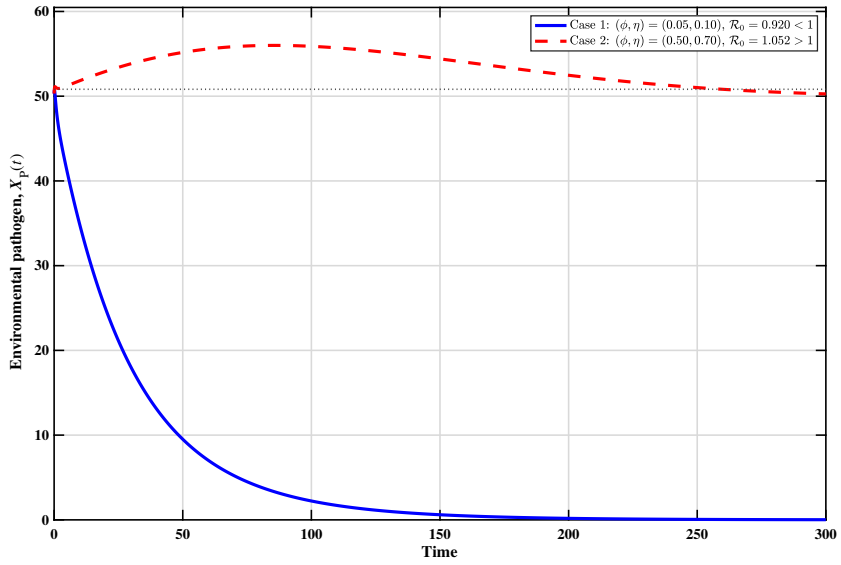
5.2. Threshold Verification in the (ϕ, η)-Plane

This subsection provides a numerical verification of the analytical threshold derived in Section 4.3. To ensure consistency with the threshold analysis, the same fixed parameter values are used. In particular, λ_P is increased from 1×10^{-5} to 1.15×10^{-5}, while all remaining parameters are fixed at their baseline values listed in Table 2. Two representative (ϕ, η) combinations are selected from opposite sides of the threshold curve in Figure 5. The corresponding temporal dynamics of the infectious population $X_I(t)$ and the environmental pathogen concentration $X_P(t)$ are presented in Figure 8. For Case 1, $(\phi, \eta) = (0.05, 0.10)$, the basic reproduction number satisfies $\Re_0 = 0.920 < 1$. Both $X_I(t)$ and $X_P(t)$ decrease monotonically toward zero, which is consistent with the global asymptotic stability of the TB-free equilibrium established analytically for $\Re_0 < 1$. By contrast, for Case 2, $(\phi, \eta) = (0.50, 0.70)$, the basic reproduction number satisfies $\Re_0 = 1.052 > 1$. In this case, the infectious population and the environmental pathogen concentration initially increase and subsequently converge to positive steady-state levels, indicating persistent TB transmission and the continued presence of the environmental reservoir. Overall, the numerical simulations agree with the analytical threshold analysis. The parameter combination below the threshold curve leads to convergence toward the TB-free equilibrium, whereas the combination above the curve leads to convergence toward an endemic equilib-

rium. Therefore, the simulations verify that the threshold curve $\eta = \eta^*(\phi)$ separates the TB-elimination and TB-persistence regions of the proposed SLIQTPR model.



(**a**)



(**b**)

Figure 8. Numerical verification of the threshold in the (ϕ, η)-plane shown in Figure 5. Temporal dynamics of (**a**) the infectious population $X_I(t)$ and (**b**) the environmental pathogen concentration $X_P(t)$. The blue solid curves correspond to Case 1, $(\phi, \eta) = (0.05, 0.10)$, for which $\mathfrak{R}_0 = 0.920 < 1$, whereas the red dashed curves correspond to Case 2, $(\phi, \eta) = (0.50, 0.70)$, for which $\mathfrak{R}_0 = 1.052 > 1$. The simulations were conducted using the same fixed parameter values as those employed in the threshold analysis in Section 4.3, including $\lambda_P = 1.15 \times 10^{-5}$.

5.3. Impact of Intervention Strategies

The effectiveness of the proposed intervention options is evaluated by numerical simulations varying one control parameter at a time while keeping fixed the baseline values of all other parameters. The effect of the primary control-related factors on TB transmission is shown in Figure 9. In panel (a), the infectious population $X_I(t)$ is significantly decreased by raising the preventive treatment rate q_L from 0.10 to 0.30 and 0.50. This implies that the total disease burden is reduced by preventing latent individuals from becoming infected with an infectious disease. Panel (b) shows the effect of increasing the treatment rate κ_I.

The infected population drops significantly with increasing κ_I from 0.20 to 0.50 to 0.80. This implies that rapid treatment of infected patients reduces infectiousness and prevents transmission. Finally, panel (c) shows the effect of the environmental pathogen clearance rate, ω. The load of the environmental pathogen $X_P(t)$ decreases as ω varies from 0.50 to 1.0 to 2.0. This points out the importance of environmental control strategies such as improved ventilation and pathogen removal in limiting indirect transmission. To summarize, the models provide evidence that improvements in environmental clearing, active treatment, and preventive treatment can reduce substantially the transmission of TB. These results underscore the importance of combining individual-based treatments with environmental control techniques and are consistent with the sensitivity analysis.

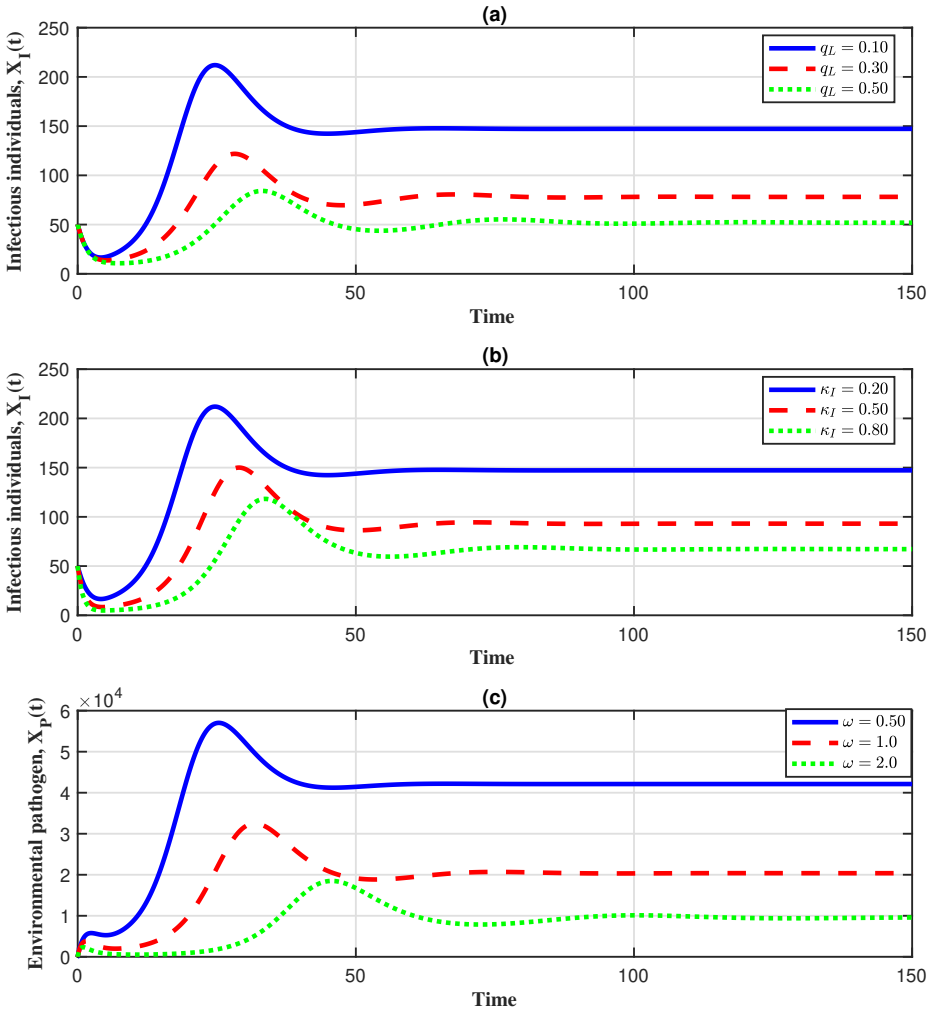


Figure 9. The impact of control-related elements on tuberculosis transmission. Panels (**a**,**b**) present the impact of raising the initiate prevention TB treatmen rate q_L, and active TB treatment rate κ_I on the infectious population $X_I(t)$, while panel (**c**) shows the effect of increasing the environmental pathogen clearance rate ω on the environmental pathogen concentration $X_P(t)$. All unspecified parameters are fixed at their baseline values in Table 2, and the initial conditions are the same that they were in the previous simulations Section 5.1.

6. Conclusions and Future Work

In this work, an SLIQTPR model was formulated and studied to incorporate direct TB transmission by infectious persons, reduced transmission by individuals under active treatment, indirect transmission through an environmental pathogen reservoir, preventative treatment of latent infection and treatment failure. The principal contribution of the model lies in combining these mechanisms within a single framework to investigate

how treatment outcomes and environmental transmission jointly affect TB elimination and persistence. The basic reproduction number, $\mathfrak{R}_0$, determines the long-term behavior of the model. When $\mathfrak{R}_0 \leq 1$, the TB-free equilibrium is globally asymptotically stable, which means that TB cannot be sustained in the population. When $\mathfrak{R}_0 > 1$, there is a unique endemic equilibrium, which is globally asymptotically stable, corresponding to ongoing transmission. Biologically, these results show that sustained TB control requires interventions capable of reducing the average number of secondary infections generated by an infectious individual to no more than one. The local and global sensitivity analyses produced broadly consistent findings, identifying recruitment, progression to active infection, environmental exposure, and pathogen shedding as important drivers of TB transmission. In contrast, susceptible mortality, preventive treatment, active treatment, and environmental pathogen clearance reduced the transmission potential. These findings emphasize the importance of strengthening preventive and active treatment programs and reducing environmental pathogen persistence.

Another important analytical result is the critical threshold relationship between treatment failure and the relative infectiousness of treated individuals. The resulting threshold curve separates the biologically feasible parameter space into disease-elimination and disease-persistence regions. This result demonstrates that treatment effectiveness cannot be evaluated solely by treatment initiation; successful control also requires reducing treatment failure and limiting residual transmission during treatment. Thus, a higher treatment failure rate requires a greater reduction in the infectiousness of treated individuals to maintain the disease below the elimination threshold. The numerical simulations are consistent with the analytical results and converged to the appropriate equilibrium with different initial conditions. The numerical simulations showed that increasing the level of preventative treatment, improving access to active treatment, and increasing the rate of removal of environmental pathogens would lead to a reduction in both the infectious population and the levels of environmental pathogens. These findings support an integrated control strategy for the management of latent TB infection, rapid and effective treatment of active TB, improved treatment outcomes, and environmental infection-control measures [3]. Nevertheless, the present results identify potential intervention mechanisms rather than provide location-specific policy recommendations. Before the model can be used to inform policy decisions, its parameters must be estimated using epidemiological and environmental data from a defined geographical setting, its initial conditions must be specified from local data, and its predictions must be validated against independent observations.

The proposed model has some limitations, which suggest directions for future research. Its parameters are assumed to be constant, and the population is considered homogeneous. Consequently, the model does not explicitly account for population movement or spatial heterogeneity. When applied to a small, approximately closed population, its quantitative outcomes would depend on local population density, contact patterns, treatment coverage, ventilation, and environmental pathogen clearance. The framework can be extended in future studies to drug-resistant TB [13], vaccination [28], reinfection [17], treatment interruption or abandonment [7,14], and spatially structured transmission [29]. Biologically reasonable delays for latent progression, diagnosis, treatment initiation, bacteriological conversion or treatment response could also be included. The analytic techniques developed for other delayed infectious disease models [30,31] could be adapted to study the effects of such delays on the persistence and stability of TB. Further extensions may include stochasticity, coinfection [32], or fractional-order dynamics [33]. Finally, optimal-control techniques may be used to find successful combinations of active treatment, preventive treatment, and environmental modifications [34,35].

Funding: This research received no external funding.

Data Availability Statement: The original contributions presented in this study are included in the article. Further inquiries can be directed to the corresponding author.

Acknowledgments: The author is grateful to the unknown referees for the many constructive suggestions, which helped to improve the presentation of the paper.

Conflicts of Interest: The author declares no conflicts of interest.

References

1. World Health Organization (WHO). *Global Tuberculosis Report 2024*; World Health Organization: Geneva, Switzerland, 2024.
2. Nardell, E. Indoor environmental control of tuberculosis and other airborne infections. *Indoor Air* **2016**, *26*, 79–87. [CrossRef] [PubMed]
3. World Health Organization (WHO). *WHO Consolidated Guidelines on Tuberculosis: Module 1: Prevention-Infection Prevention and Control*; World Health Organization: Geneva, Switzerland, 2022.
4. Médecins Sans Frontières; Partners in Health. *Tuberculosis*. MSF Medical Guidelines. 2025. Available online: https://medicalguidelines.msf.org/en/viewport/TUB/english/tuberculosis-20321086.html (accessed on 30 June 2026).
5. Liu, J.; Zhang, T. Global stability for a tuberculosis model. *Math. Comput. Model.* **2011**, *54*, 836–845. [CrossRef]
6. Yang, Y.; Li, J.; Ma, Z.; Liu, L. Global stability of two models with incomplete treatment for tuberculosis. *Chaos Solitons Fractals* **2010**, *43*, 79–85. [CrossRef]
7. Liu, L.; Wang, Y. A mathematical study of a TB model with treatment interruptions and two latent periods. *Comput. Math. Methods Med.* **2014**, *2014*, 932186. [CrossRef] [PubMed]
8. Ullah, I.; Ahmad, S.; Al-Mdallal, Q.; Khan, Z.A.; Khan, H.; Khan, A. Stability analysis of a dynamical model of tuberculosis with incomplete treatment. *Adv. Differ. Equ.* **2020**, *2020*, 499. [CrossRef]
9. Barrios, E.; Bastidas-Santacruz, H.E.; Ramírez Bernate, C.A.; Vasilieva, O. A synthesized model of tuberculosis transmission featuring treatment abandonment. *Math. Biosci. Eng.* **2022**, *19*, 11018–11037. [CrossRef] [PubMed]
10. Onuorah, J.O.; Nsabimana, W.; Onuorah, M.O. A Compartmental Mathematical Model for Tuberculosis Transmission Incorporating Antibiotic Resistance and Treatment Failures. *ULK Sci. J.* **2025**, *46*. Available online: https://www.researchgate.net/publication/395732293 (accessed on 30 June 2026).
11. Aldila, D. Change in stability direction induced by temporal interventions: A case study of a tuberculosis transmission model with relapse and reinfection. *Front. Appl. Math. Stat.* **2025**, *11*, 1541981. [CrossRef]
12. Garba, U.; Azmi, A.; Mohd, M.H.; Artes, R.G., Jr. Mathematical Modeling of Tuberculosis Transmission Dynamics with Vaccination and Drug Resistance. *Malays. J. Fundam. Appl. Sci.* **2025**, *21*, 2513–2537. [CrossRef]
13. Wang, L.; Teng, Z.; Rifhat, R.; Wang, K. Modelling of a drug resistant tuberculosis for the contribution of resistance and relapse in Xinjiang, China. *Discret. Contin. Dyn. Syst.-Ser. B* **2023**, *28*, 4167–4189. [CrossRef]
14. Ochieng, F.O. Mathematical modeling of tuberculosis transmission dynamics with reinfection and optimal control. *Eng. Rep.* **2025**, *7*, e13068. [CrossRef]
15. Zhang, J.; Takeuchi, Y.; Dong, Y.; Peng, Z. Modelling the preventive treatment under media impact on tuberculosis: A comparison in four regions of China. *Infect. Dis. Model.* **2024**, *9*, 483–500. [CrossRef] [PubMed]
16. Zhao, K.; Liu, Z.; Guo, C.; Xiang, H.; Liu, L.; Wang, L. Modeling and analysis of transmission dynamics of tuberculosis with preventive treatment and vaccination strategies in China. *Appl. Math. Model.* **2025**, *138*, 115779. [CrossRef]
17. Li, Q.; Wang, F. An epidemiological model for tuberculosis considering environmental transmission and reinfection. *Mathematics* **2023**, *11*, 2423. [CrossRef]
18. Yulida, Y.; Suhartono, E.; Anggraini, D.; Arifin, S. Mathematical models of tuberculosis disease and environmental factors: A systematic review. *Pak. J. Life Soc. Sci.* **2024**, *22*, 4116–4130.
19. Ochieng, F.O. SEIRS model for TB transmission dynamics incorporating the environment and optimal control. *BMC Infect. Dis.* **2025**, *25*, 490. [CrossRef] [PubMed]
20. World Health Organization (WHO). *WHO Operational Handbook on Tuberculosis. Module 1: Prevention-Tuberculosis Preventive Treatment*; World Health Organization: Geneva, Switzerland, 2024.
21. World Health Organization (WHO). *WHO Consolidated Guidelines on Tuberculosis. Module 4: Treatment and Care*; World Health Organization: Geneva, Switzerland, 2025.
22. Peter, O.J.; Aldila, D.; Ayoola, T.A.; Balogun, G.B.; Oguntolu, F.A. Modeling tuberculosis dynamics with vaccination and treatment strategies. *Sci. Afr.* **2025**, *28*, e02647. [CrossRef]
23. Van den Driessche, P.; Watmough, J. Reproduction numbers and sub-threshold endemic equilibria for compartmental models of disease transmission. *Math. Biosci.* **2002**, *180*, 29–48. [CrossRef] [PubMed]
24. La Salle, J.P. *The Stability of Dynamical Systems*; SIAM: Philadelphia, PA, USA, 1976.

25. Smith, H.L.; Waltman, P. *The Theory of the Chemostat: Dynamics of Microbial Competition*; Cambridge University Press: Cambridge, UK, 1995; Volume 13.
26. Lee, J.Y. Tuberculosis Infection Control in Health-Care Facilities: Environmental Control and Personal Protection. *Tuberc. Respir. Dis.* **2016**, *79*, 234–240. [CrossRef] [PubMed]
27. Marino, S.; Hogue, I.B.; Ray, C.J.; Kirschner, D.E. A methodology for performing global uncertainty and sensitivity analysis in systems biology. *J. Theor. Biol.* **2008**, *254*, 178–196. [CrossRef] [PubMed]
28. Oshinubi, K.; Peter, O.J.; Addai, E.; Mwizerwa, E.; Babasola, O.; Nwabufo, I.V.; Sane, I.; Adam, U.M.; Adeniji, A.; Agbaje, J.O. Mathematical modelling of tuberculosis outbreak in an East African country incorporating vaccination and treatment. *Computation* **2023**, *11*, 143. [CrossRef]
29. Amiri, L.; Torabi, M.; Deardon, R.; Pickles, M. Spatial modeling of individual-level infectious disease transmission: Tuberculosis data in Manitoba, Canada. *Stat. Med.* **2021**, *40*, 1678–1704. [CrossRef] [PubMed]
30. Almuallem, N.A. Global properties of a delayed model for the dynamics of lumpy skin disease with vaccination efficacy. *AIMS Math.* **2025**, *10*, 20642–20669. [CrossRef]
31. Elaiw, A.M.; Almuallem, N.A. Global properties of delayed-HIV dynamics models with differential drug efficacy in cocirculating target cells. *Appl. Math. Comput.* **2015**, *265*, 1067–1089. [CrossRef]
32. Ali Shah, S.M.; Nie, Y.; Din, A.; Alkhazzan, A.; Younas, B. Stochastic modeling and analysis of Hepatitis and Tuberculosis co-infection dynamics. *Chin. Phys. B* **2024**, *33*, 110203. [CrossRef]
33. El-Mesady, A.; Mahdy, A.; Özköse, F. A fractional–order model with prevention and isolation optimal control measures to reduce the transmission of Tuberculosis. *J. Taibah Univ. Sci.* **2025**, *19*, 2475579. [CrossRef]
34. Li, Y.; Liu, X.; Yuan, Y.; Li, J.; Wang, L. Global analysis of tuberculosis dynamical model and optimal control strategies based on case data in the United States. *Appl. Math. Comput.* **2022**, *422*, 126983. [CrossRef]
35. Peter, O.J.; Abidemi, A.; Fatmawati, F.; Ojo, M.M.; Oguntolu, F.A. Optimizing tuberculosis control: A comprehensive simulation of integrated interventions using a mathematical model. *Math. Model. Numer. Simul. Appl.* **2024**, *4*, 238–255. [CrossRef]

Disclaimer/Publisher's Note: The statements, opinions and data contained in all publications are solely those of the individual author(s) and contributor(s) and not of MDPI and/or the editor(s). MDPI and/or the editor(s) disclaim responsibility for any injury to people or property resulting from any ideas, methods, instructions or products referred to in the content.